8-2013

PROBABILISTIC BACK ANALYSIS OF GEOTECHNICAL SYSTEMS

Lei Wang
Clemson University, lwang6@g.clemson.edu

PROBABILISTIC BACK ANALYSIS OF GEOTECHNICAL SYSTEMS

A Thesis
Presented to
the Graduate School of
Clemson University

In Partial Fulfillment
of the Requirements for the Degree
Master of Science
Civil Engineering

---

by
Lei Wang
August 2013

Accepted by:
Dr. C. Hsein Juang, Committee Chair
Dr. Sez Atamturktur, Co-Chair
Dr. Weichiang Pang
Dr. Yongxi Huang

ABSTRACT

This thesis is aimed at applying the probabilistic approaches for back analysis of geotechnical systems. First, a probabilistic back-analysis of a recent slope failure at a site on Freeway No. 3 in northern Taiwan is presented. The Markov Chain Monte Carlo (MCMC) simulation is used to back-calculate the geotechnical strength parameters and the anchor force. These inverse analysis results, which agree closely with the findings of the post-event investigations, are then used to validate the maximum likelihood method, a computationally more efficient back-analysis approach. The improved knowledge of the geotechnical strength parameters and the anchor force gained through the probabilistic inverse analysis better elucidate the slope failure mechanism, which provides a basis for a more rational selection of remedial measures.

Then the maximum likelihood principle is adapted to formulate an efficient framework for probabilistic back analysis of soil parameters in a braced excavation using multi-stage observations. The soil parameters are updated using the observations of the maximum ground settlement and/or wall deflection measured in a staged excavation. The updated soil parameters are then used to refine the predicted wall and ground responses in the subsequent excavation stages, as well as to assess the building damage potential at the final excavation stage. Case study shows that the proposed approach is effective in improving the predictions of the excavation-induced wall and ground responses. More-accurate predictions of the wall and ground responses, in turn, lead to a more accurate assessment of the damage potential of buildings adjacent to the excavation.

DEDICATION

This thesis is dedicated to my parents. This thesis exists because of their love and support.

ACKNOWLEDGMENTS

I would like to express my sincere thanks to my advisors, Dr. C. Hsein Juang and Dr. Sez Atamturktur, for their invaluable advice, support and encouragement all along completing this work. I am grateful to other committee members: Dr. Weichiang Pang and Dr. Yongxi Huang. They were all supportive and actively helped in the completion of the thesis. I would also like to thank Dr. Ronald Andrus and Dr. Nadarajah Ravichandran for their help during the course of my study at Clemson.

I am grateful to Zhifeng Liu, Zhe Luo, Wenping Gong, Bin Pei for engaging discussion and for their friendship. I am also grateful to Biao Li, Jinying Zhu, Mengxin Song, Hao Hao for their support.

Finally, I would like to thank my parents for their enduring support and encouragement through my education.

The study is funded by Glenn Department of Civil Engineering, Clemson University. I also wish to thank the Shrikhande family and the Glenn Department of Civil Engineering for awarding me the Aniket Shrikhande Memorial Annual Graduate Fellowship.

TABLE OF CONTENTS

Table of Contents (Continued)

Page

LIST OF TABLES

LIST OF FIGURES

List of Figures (Continued)

Figure Page

CHAPTER ONE

INTRODUCTION

Motivation and Background

Uncertainties in the parameters of earthen materials have long been recognized (Christian et al. 1994; Phoon and Kulhawy 1999). To deal with these uncertainties, the probabilistic or reliability-based approach that considers explicitly the uncertainties in the geotechnical parameters has been proposed (e.g., Wu et al. 1989; Christian et al. 1994; Duncan 2000; Baecher and Christian 2003; Phoon et al. 2003; Shou et al. 2005; Hsiao et al. 2008; Najjar and Gilbert 2009; Juang et al. 2011; Lee et al. 2012). The results of the probabilistic analysis are realistic only if the input parameters can be well characterized statistically. Thus, the challenge of the probabilistic approach lies in determining the probability distribution of input parameters, which is quite challenging since in a typical project, available data is often very limited (Gilbert et al. 1998; Baecher and Christian 2003; Hoek 2006; Lee et al. 2012). In geotechnical engineering, it is often desirable to back analyze the input parameters based on field observations to improve statistical characterization on the input parameters.

Past work on back analysis of geotechnical system is primarily based on deterministic approach, with which the calibration parameters are assumed to be "non-random" and the analysis model is assumed to be "error-free" (i.e., no model error). For example, in the deterministic back analysis, the solutions obtained through the deterministic analysis are often matched with field observations of the geotechnical

system (e.g., Ou and Tang 1994; Tang et al. 1999; Calvello and Finno 2004; Rechea et al. 2008; Stark et al. 2008; Hashash et al. 2010). However, the deterministic back analysis techniques simply neglect the uncertainty in the input parameters (e.g., the key soil parameters) that are generally high (Harr 1987; Phoon and Kulhawy 1999; Hsiao et al. 2008; Lee et al. 2012). It is reported that the uncertainty in soil parameters has a significant influence on the predicted response of geotechnical systems (Hsiao et al. 2008; Wang et al. 2010; Zhang et al. 2011).

In this regard, it is desirable to perform the probabilistic back analysis of geotechnical systems to improve one's knowledge on the parameters of a geotechnical model based on field observations. This thesis focuses on developing an efficient probabilistic back analysis framework for geotechnical problems such as slope failure and braced excavation. Chapter II of this thesis is devoted to develop efficient procedures for probabilistic back analysis of slope failure based on the Maximum Likelihood principle and the Markov Chain Monte Carlo simulation. The improved knowledge of the geotechnical strength parameters and the anchor force gained through the probabilistic back analysis can better elucidate the slope failure mechanism, which provides a basis for a more rational selection of remedial measures. Chapter III of this thesis further formulates an efficient procedure based on the maximum likelihood principle for probabilistic back analysis of braced excavations. The soil parameters are updated using the observations of the maximum ground settlement and/or the maximum wall deflection measured in a staged excavation. The updated soil parameters are then used to refine the

predicted wall and ground responses in the subsequent excavation stages, as well as to assess the building damage potential at the final excavation stage.

Objectives and Thesis Organization

The scope of this thesis focuses on the application of probabilistic back analysis methods in geotechnical systems. The first objective of this thesis is to establish a Markov Chain Monte Carlo (MCMC) simulation-based framework for the probabilistic back analysis of slope failure. The second objective of this thesis is to develop an efficient probabilistic back analysis framework for slope failure based on the maximum likelihood principle and validate this framework with MCMC simulation results. The third objective of this thesis is to develop an efficient framework based on the maximum likelihood principle for back analysis of soil parameters in braced excavations using multi-stage observations.

This thesis consists of four chapters. In Chapter I, an introduction is presented that sets the outline and stage for the entire thesis. Chapter II and Chapter III present major contents of the thesis work. In Chapter II, a probabilistic back analysis of a recent slope failure in northern Taiwan is presented. In Chapter III, an efficient framework based on the maximum likelihood principle for back analysis of soil parameters in a staged excavation using field observations is proposed and demonstrated with a case study. Finally, in Chapter IV, the last chapter, the main conclusions of this thesis are presented.

CHAPTER TWO

PROBABILISTIC BACK ANALYSIS OF SLOPE FAILURE

Introduction

The experience-calibrated factor of safety (FS) approach is traditionally used in the slope stability analysis. To account for the uncertainty in geotechnical parameters explicitly, however, probabilistic methods are often used (Christian et al. 1994; Juang et al. 1998; Duncan 2000; Park et al. 2005; Shou et al. 2005; Penalba et al. 2009; Wang et al. 2010; Li et al. 2011; Lee et al. 2012; Park et al. 2012a; Park et al. 2012b; Wang et al. 2012). The accuracy of the probabilistic analysis depends on the proper statistical characterization of the input parameters. However, a proper statistical characterization of the input parameters often requires testing of a large number of samples extracted from a wide range of sites in question. In a routine geotechnical practice, available data is often very limited (Gilbert et al. 1998; Hoek 2006). Apart from the uncertainties of the geotechnical parameters, the uncertainty and deterioration of anchors in a slope system are often more difficult to estimate (Xanthakos 1991).

In a deterministic approach, the back-analysis of geotechnical strength parameters is usually determined through a trial-and-error process, in which various values for geotechnical strength parameters and slip angles are assumed and analyzed until the input

---

[*]A similar form of this chapter has been published at the time of writing: Wang L, Hwang JH, Luo Z, Juang CH, Xiao J. (2013). Probabilistic back analysis of slope failure – a case study in Taiwan. Computers and Geotechnics, 51, 12-23.

values that yield FS = 1 are obtained (Tang et al. 1999; Stark et al. 2008). The deterministic approach is, however, inadequate for addressing the uncertainties in the estimated geotechnical strength parameters. In this study, a framework for a probabilistic back analysis of input parameters of a slope stability model based on field observations in a slope failure event is adopted. The improved knowledge on the input parameters through this probabilistic back analysis contributes to the safety evaluation, updating analysis, and remedial design of the slope (Tang et al. 1999; Zhang et al. 2011).

In this chapter, two approaches for the probabilistic back analysis of slope failure are adopted by the author for a case study of rock slope failure at Freeway No. 3 in Taiwan (TGS 2011). The first approach employs a Markov Chain Monte Carlo (MCMC) simulation-based framework for the inverse analysis of the slope failure at Freeway No 3. This time-consuming procedure is generally capable of simulating uncertainty parameters and producing accurate results. The second approach involves a Maximum Likelihood (ML)-based optimization algorithm that can be easily implemented in a user-friendly spreadsheet environment. The ML-based approach requires much less computational effort and thus has a greater potential as a tool in the geotechnical engineering practice.

With this enhanced knowledge of the input parameters for the slope system, it is possible to elucidate the failure mechanism to create a more reasonable estimate of the failure probability of the slope. This improved knowledge of input parameters, coupled with the reliability-based design approach, provides a more rational approach for selecting suitable measures to mitigate slope failures.

Overview of the 2010 Landslide on Freeway No. 3, Taiwan

The Freeway No. 3 Landslide occurred at approximately 14:29 p.m. on April 25, 2010 (local time) at the 3k+300m location of Freeway No. 3 on the Sai Gong Gek mountain, approximately 20 kilometers northeast of Taipei, the capital of Taiwan. In this landslide, approximately half of the hill gave way, in which more than 200,000 m^3 of dirt and rocks crashed onto the motorway and destroyed an overpass, resulting in a road closure and blockage of this 6-lane freeway between Keelung and Taipei (TGS 2011; Hsiao et al. 2011). A panoramic view of this landslide is shown in Figure 2.1(a) and 2.1(b), in which the sliding mass may be approximated as a triangular sliding mass. The base width of the triangular sliding mass (along the Freeway No. 3) is approximately 155 m and the length of two sides of the triangular sliding mass is about 185 m (TGS 2011). At the time of landslide, it was a sunny day and no tremors occurred, thus excluding both heavy rainfall and earthquake, the two major causes of landslides in Taiwan, as the causes of failure.

The site of collapsed rock slope is located in the Miocene Taliao formation. The geological map shows a sedimentary rock formation of shale, sandstone, alternation of sandstone and shale in this site. The geological profile of the slope mainly consists of six layers as shown in Figure 2.2. It is noted that in this area, the strike of rock formation is in the NE direction, and the dip slopes are in the SE direction at an angle of $10^o - 30^o$. Because of these rock slope characteristics, and the fact that Freeway No. 3 cut through the dip slope, there was a high potential for a dip-slope failure.

Figure 2.1: Site photograph of the Freeway No.3 landslide in Taiwan: (a) Panoramic view; (b) Another view (National Airborne Service Corps, Ministry of Interior, Taiwan, 2011, http://www.nasc.gov.tw/)

The top layer is an overburden soil layer with a thickness of 2-5 m, and the second layer is a sandstone (SS) layer with a thickness of approximately 10 m, which is interspersed with laminate shale and with vertical tension joints slid downward. The third layer consists of alternations of thin sandstone and shale (SS/SH) with an approximate thickness of 1 m, and the fourth layer is a dark gray shale (SH) with an approximate thickness of 6 m with laminate siltstones. The fifth and sixth layers are sandstone with an approximate thickness of 2-3 m with significant trace of fossil (SS-f) on the bedding plane, and alternating layers of thin sandstone and shale (SS/SH), respectively. The sliding plane is close to the interface of the third and fourth layers on top of the dark gray shale. During rock boring, clay seams, which had been suspected as a potential cause for dip slope failure, were found at the depth of the sliding plane within some boreholes.

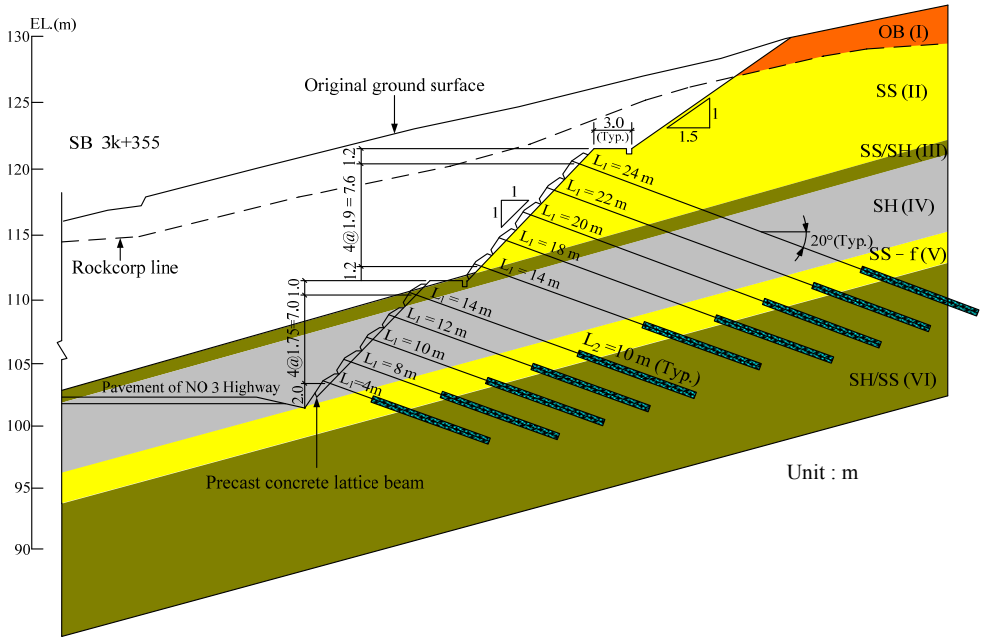

Figure 2.2: Geometry and geological profile of a cross-section of the collapsed slope on Freeway No.3

The rock slope at Freeway No. 3 landslide site is geometrically classified as a dip slope with an easy flow direction surface that contains a shale and sandstone interlayer with a high porosity. During the construction of Freeway No. 3, the foot of the dip slope was excavated and 572 rock anchors (or bolts) were installed to support the slope. The horizontal spacing of the anchors was approximately 2.6 m and the vertical spacing of the anchors was approximately 1.8 m (TGS 2011). The construction of the anchor system was completed in 1998. Field investigations after the slope failure (April 2010) showed that only 58 anchors remained in place after the slope failure. Forty-eight percent (48%) of the remaining anchors showed a fracture of steel strands (TGS 2011).

Post-event field measurements by the authors indicate an average slip surface of inclination of 15°. In fact, the measured slip surface of inclination in various areas of the slip surface is in the range of 14° to 16°. These observations are consistent with independent post-event failure investigation and analysis by Chen et al. (2010) and Lin et al. (2010), which reported a slip surface of inclination of 14° and 15°, respectively.

Deterministic Model for Rock Slope Stability Analysis

The location of the slip surface was determined from a site investigation, which may be simplified as a single plane failure surface as indicated in Figure 2.3. The rock slope stability analysis may be obtained through the use of a deterministic model such as that developed by Hoek and Bray (1981). This model is a limit equilibrium analytical model for plane failure. The slope stability was determined by a factor of safety (FS),

defined as the ratio of the forces resisting sliding to the forces tending to induce sliding along the slip surface (Hoek and Bray 1981; Turner and Schuster 1996; Wyllie and Mah 2004):

$$FS = \frac{cA + [W\cos(\eta) - U - V\sin(\eta) + T\cos(\theta)]\tan\phi}{W\sin(\eta) + V\cos(\eta) - T\sin(\theta)} \tag{2.1}$$

where c is the cohesive strength along sliding surface (ton/m^2); ϕ is the friction angle of sliding surface (°); A is the area of slip (or shear) plane (m^2); θ is the angle between the rock anchor and normal vector of slip surface (°); η is the angle of slip surface (°); W is the weight of slipped volume (ton); U is the uplift force due to water pressure on the failure surface (ton); V is the horizontal force due to water in the tension crack (ton); T is the summation of design forces of all rock anchors (ton).

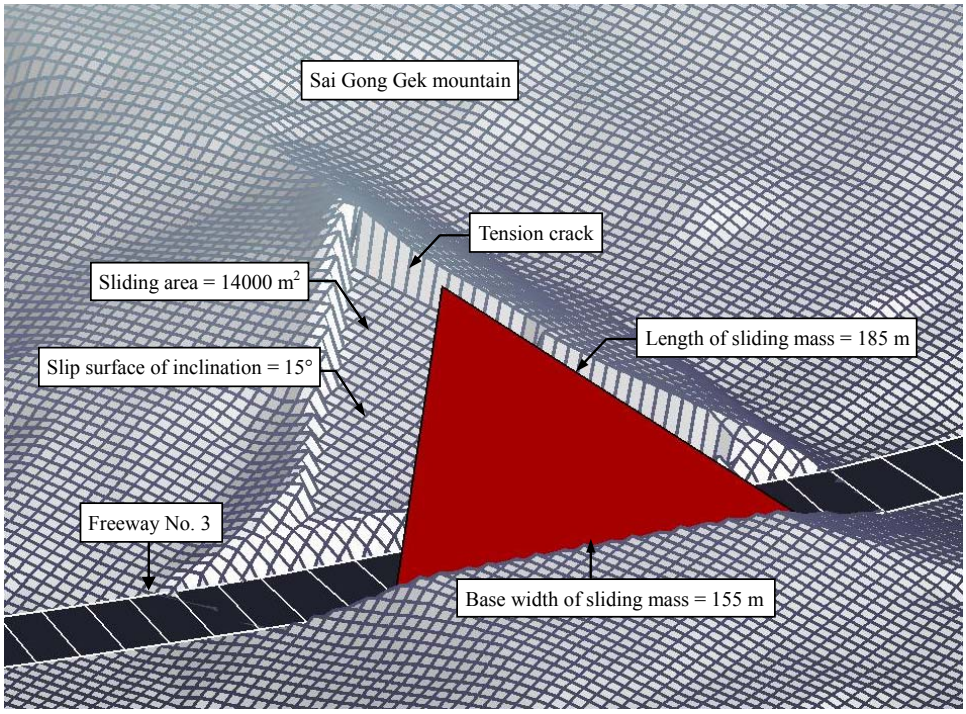

Figure 2.3: 3-D illustration of the collapsed slope on Freeway No.3

It should be noted that in the case study presented later, Eq. (2.1) was not used to analyze a single specific section of a 3-D sliding mass. The entire sliding rock mass was treated rather as a single unstable block, with Eq. (2.1) being used to analyze this 3-D sliding mass. This 3-D analysis nature can be detected by observing the units of the variables in Eq. (2.1). For example, the unit for the area of the slip plane is "m^2" instead of "m^2/m" or "m"; and the unit for the weight of the slipped rock mass is "ton" instead of "ton/m". It is quite common in rock engineering (Turner and Schuster 1996) to analyze the stability of a rock slope in 3-D using Eq. (2.1). The back-analyzed rock properties, presented later, refer rather to the average properties along the entire failure surface in the actual 3-D space, not the properties along a single specific section.

In a deterministic analysis, slope failure is said to occur if FS ≤ 1. Thus, in theory FS at the moment of failure is unity (Duncan and Wright 2005; Zhang et al. 2010a). This concept is usually used in the back analysis of slope stability, particularly for use in any post-event investigation.

Based on the TGS report (TGS 2011), the groundwater table during the slope failure at the site of case study (Freeway No.3) was located at a great depth and not within the slope stability analysis domain. In addition, there was practically no precipitation for at least 15 days before the failure event, thus making it reasonable to assume that U and V were zero in the analysis. The detailed parameter values in this deterministic analysis of the stability of Freeway No.3 site slope are summarized in Table 2.1. These data are used in the back-analysis presented in the subsequent sections. It should be noted that the back-analyzed geotechnical property in this case mainly refers to

the shear strength along the slip surface (in terms of the internal friction angle ϕ), which is an average effect of the shear properties of sandstone, shale and clay seams along the interface between the third and fourth layers.

Table 2.1: Parameter values for the deterministic analysis of the stability of Freeway No. 3 slope (adapted from Hsiao et al. 2011 and TGS 2011)

Parameter	Value
Unit weight of rock, γ_r (ton/m^3)	2.1
Volume of slipped rock, V_r (m^3)	225078.5
Weight of slipped rock, W (ton)	472664.9
Anchor force of single anchor (ton)	60
Number of anchors	572
Inclined angle of anchor, θ (°)	55
Cohesion, c (kg/cm^2)	0
Dip angle of slip surface, η (°)	15
Area of slip plane, A (m^2)	14000

Back Analysis of Strength Parameter and Anchor Load

Markov Chain Monte Carlo (MCMC) technique

The prior information of uncertain parameters is provided in Table 2.2. The mean value of the internal friction angle ϕ was estimated from limited testing data of samples taken at the slip surface in the post-event investigation, and the COV of ϕ was estimated based on those reported in the literature (Lee et al. 2012). The mean anchor force was the initial design value of this anchor system, and the COV of the anchor force was estimated at 38% based upon the results of the field tests reported by Li et al. (2007) and Zhang et al. (2009).

Table 2.2: Statistics of uncertain parameters (adapted from TGS 2011)

Parameter	Mean	Std. dev.	COV
ϕ (°)	21	3.15	0.15
T (ton)	60	22.8	0.38

The procedure developed by Zhang et al. (2010a) was adapted for back-analysis of the slope stability of Freeway No 3 slope. The model for analyzing this slope stability is expressed as:

$$y = g(\boldsymbol{\theta}) + \varepsilon \tag{2.2}$$

where y is the observed factor of safety; $g(\boldsymbol{\theta})$ denotes the calculated factor of safety using Eq.(2.1); and $\boldsymbol{\theta}$ is the vector of the input parameters of the model (ϕ and T). The error term ε, assumed as statistically independent with the observation, follows a normal distribution with a mean μ_ε and a standard deviation σ_ε.

The occurrence of this slope failure theoretically implies that the observed factor of safety is equal to unity. Thus, the likelihood of the factor of safety (y) being equal to the observation of slope failure (FS = 1) is the conditional probability density function (PDF) of $\boldsymbol{\theta}$, expressed as:

$$L(\boldsymbol{\theta} \mid Failure) = \phi\left[\frac{g(\boldsymbol{\theta}) + \mu_\varepsilon - 1}{\sigma_\varepsilon}\right] \tag{2.3}$$

According to the Bayesian inference methodology, the posterior PDF is proportional to the product of the likelihood function and the prior distribution (Ang and

Tang 2007):

$$f(\boldsymbol{\theta} \mid Failure) = k\,\phi\left[\frac{g(\boldsymbol{\theta}) + \mu_{\varepsilon} - 1}{\sigma_{\varepsilon}}\right] f(\boldsymbol{\theta}) \tag{2.4}$$

where k is a normalization constant and $f(\boldsymbol{\theta})$ is the prior distribution. The posterior distribution was obtained using sampling methods such as the Markov Chain Monte Carlo (MCMC) simulation technique. Here, we used the Metropolis-Hastings algorithm (Metropolis et al. 1953; Hastings 1970) to construct the Markov chains for the back-analysis of Freeway No. 3 Slope, the details of which are listed below (with reference to Figure 2.4). In this procedure:

1. The term $\boldsymbol{\theta}_0$ is randomly selected in the Markov chain.
2. For the k^{th} iteration, the k+1 point $\mathbf{Y}$ is generated from a proposal distribution $J(\mathbf{Y}|\boldsymbol{\theta}_k)$, that is determined as a multivariate normal distribution with a mean of $\boldsymbol{\theta}_k$ and a covariance matrix of $\xi \cdot \mathbf{C}_{\boldsymbol{\theta}}$ where ξ is a scaling factor and $\mathbf{C}_{\boldsymbol{\theta}}$ is the covariance matrix of the prior distribution of $\boldsymbol{\theta}$.
3. A random number U is generated from a uniform distribution (0, 1).
4. Accept $\mathbf{Y}$ as $\boldsymbol{\theta}_{k+1}$ with a probability:

$$r = \min\left[1,\ \frac{q(\boldsymbol{\theta}_k|\mathbf{Y})}{q(\mathbf{Y}|\boldsymbol{\theta}_k)}\right] \tag{2.5}$$

$q(\boldsymbol{\theta}|\mathbf{Y})$ is the un-normalized posterior PDF adapted from Eq. (2.4). If $U < r$,

then accept the new point $\mathbf{Y}$ and set $\boldsymbol{\theta}_{k+1} = \mathbf{Y}$, else reject $\mathbf{Y}$ and set $\boldsymbol{\theta}_{k+1} = \boldsymbol{\theta}_k$.

5. The iteration is halted if k reaches the pre-specified number of samples (i.e., Markov chain "length").

We note that the initial samples acquired during the initial phase of the Markov Chain obtained from the Metropolis-Hastings algorithm are unstable and should be discarded (Juang et al. 2013). The number of these discarded, or "burn in" samples, depends on a specific problem. In this study, the number was 500, based upon a trial and error process for obtaining converged results.

Back analysis using MCMC – Case study

For demonstration purposes, the prior distributions of ϕ and T were assumed to follow a lognormal distribution with the statistics listed in Table 2.2. The model error ε was assumed to follow a normal distribution with mean $\mu_\varepsilon = 0.05$ and standard deviation $\sigma_\varepsilon = 0.07$ following the study by Zhang et al. (2011). It should be noted that the normal distribution assumption for this model error may be only suitable for this specific slope problem based on the study by Zhang et al. (2011); for other geotechnical problems, a different distribution (e.g., lognormal distribution) may be more appropriate.

To study the effect of the scaling factor ξ, the Markov chains of friction angle were first simulated at three different ξ values (0.005, 1 and 100), the results of which are shown in Figure 2.5. Here, the Markov Chain length, in terms of number of samples drawn from each simulation, is 10,000.

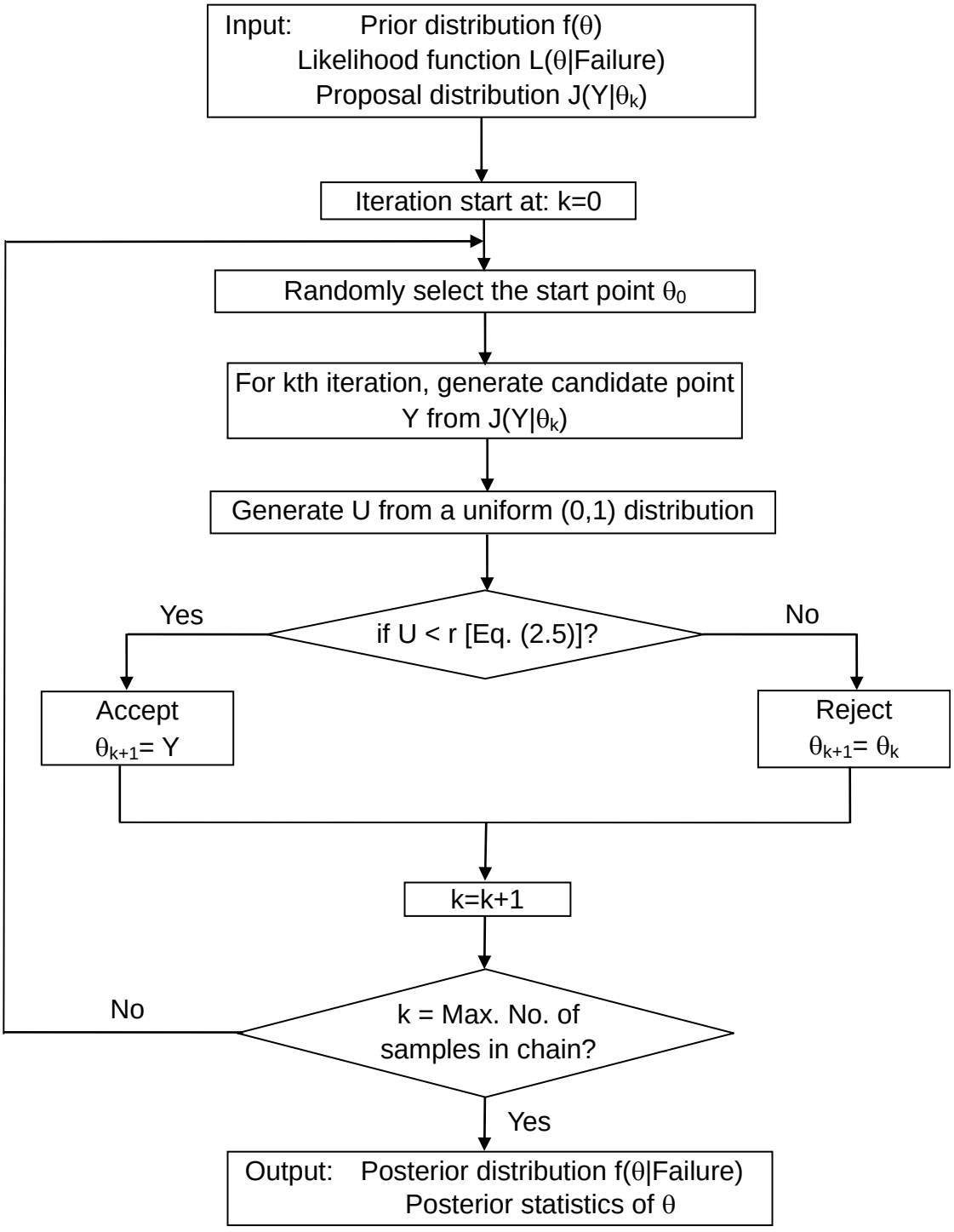

Figure 2.4: Flowchart for back analysis with Markov Chain Monte Carlo framework

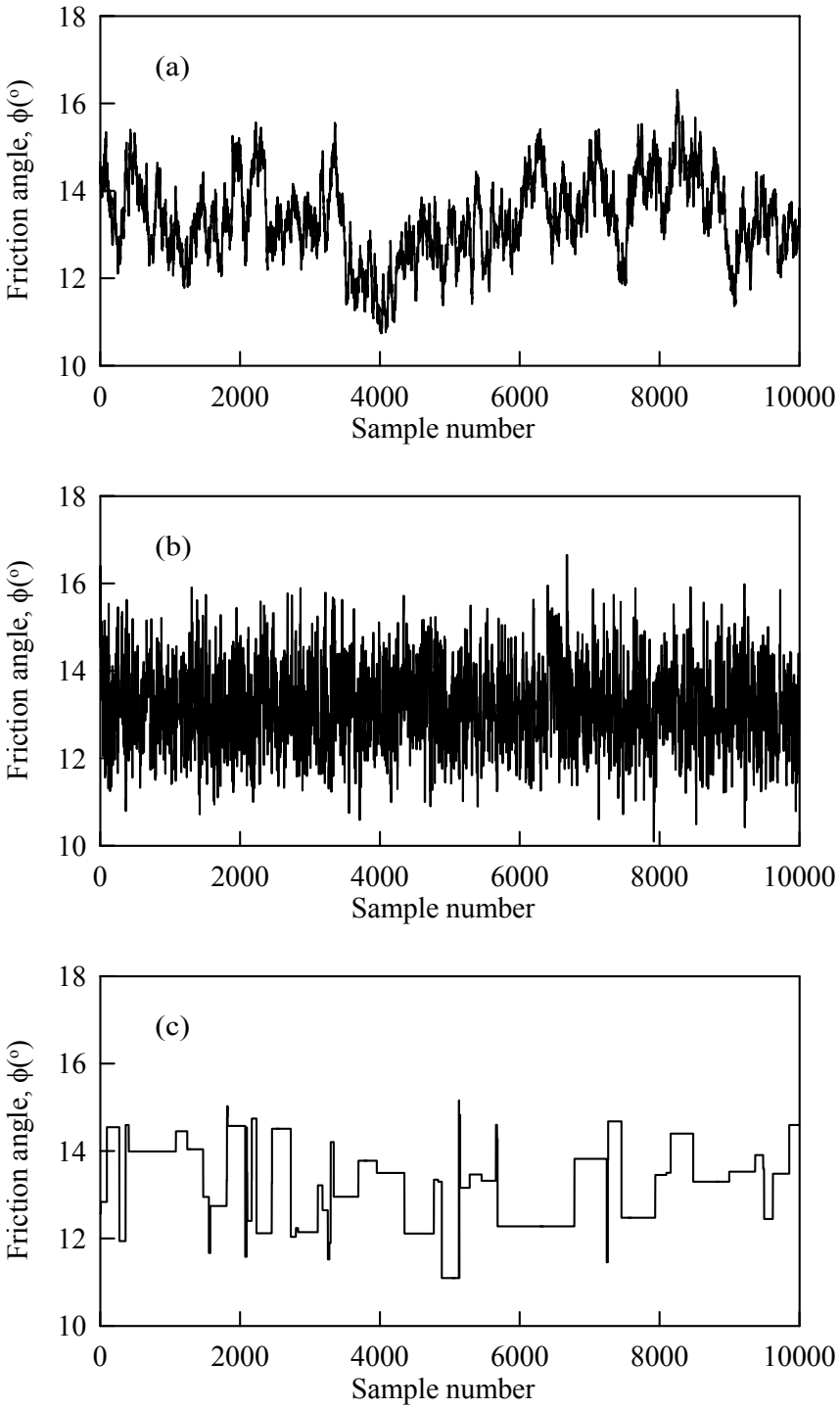

Figure 2.5: Effects of ξ on the samples for ϕ in a Markov chain: (a) $\xi = 0.005$; (b) $\xi = 1$; (c) $\xi = 100$

Table 2.3: Means and standard deviations of posterior statistics of input parameters from 10 Markov chains with $\xi = 0.005$

Number of samples	Statistics	Mean of ϕ (°)	Std. dev. of ϕ (°)	Mean of T (ton)	Std. dev. of T (ton)
10000	Mean	13.16	0.94	35.68	9.59
	Std. dev.	0.24	0.08	2.84	1.04
40000	Mean	13.23	0.91	34.83	9.52
	Std. dev.	0.08	0.03	1.11	0.77
60000	Mean	13.25	0.94	34.95	9.84
	Std. dev.	0.07	0.04	0.90	0.61

Table 2.4: Means and standard deviations of posterior statistics of input parameters from 10 Markov chains with $\xi = 1$

Number of samples	Statistics	Mean of ϕ (°)	Std. dev. of ϕ (°)	Mean of T (ton)	Std. dev. of T (ton)
10000	Mean	13.20	0.93	35.38	9.79
	Std. dev.	0.02	0.02	0.31	0.20
40000	Mean	13.21	0.93	35.30	9.78
	Std. dev.	0.01	0.01	0.12	0.09
60000	Mean	13.21	0.93	35.29	9.81
	Std. dev.	0.01	0.01	0.11	0.11

Table 2.5: Means and standard deviations of posterior statistics of input parameters from 10 Markov chains with $\xi = 100$

Number of samples	Statistics	Mean of ϕ (°)	Std. dev. of ϕ (°)	Mean of T (ton)	Std. dev. of T (ton)
10000	Mean	13.19	0.92	36.11	9.66
	Std. dev.	0.15	0.09	1.99	0.77
40000	Mean	13.19	0.95	35.68	10.14
	Std. dev.	0.07	0.05	0.79	0.87
60000	Mean	13.19	0.94	35.25	9.89
	Std. dev.	0.07	0.06	0.73	0.68

As show in Figure 2.5, when ξ is too small (ξ=0.005), the Markov chain moves quite slowly, requiring a large amount of time to move from one side of the posterior space to the other. When ξ is too large (ξ=100), the sampled points are frequently rejected, resulting in a "flat" plot in Figure 2.5(c), which indicates the efficiency of the MCMC is low. When ξ=1, the sampled points actively move through the effective parameter ranges, which is considered to be more effective.

The effects of various scaling factor ξ and number of samples on the posterior statistics of input parameters are shown in Table 2.3 to Table 2.5, detailing how ten repeated Markov chains were drawn consecutively to illustrate the variance in the estimated posterior statistics. Here, an increase in the Markov chain length (number of samples in the Markov chain), resulted in a significant reduction of the variation in the estimated statistics (mean and standard deviation), thus yielding more converged results. Furthermore, a comparison of these tables shows that a nearly identical mean value of both statistics is obtained regardless of the ξ values. The variation in the estimated statistics is smallest when ξ=1, indicating that more converged outcomes (i.e., statistics of the posterior distributions) can be achieved with ξ=1.

The proper scaling factor ξ was selected based upon the acceptance ratio, which is defined as the ratio of accepted sample number to the total sample number. For the maximum efficiency of the Markov chain, Gelman et al. (2004) recommend an acceptance ratio between approximately 20%-40%. The plot of ξ values against the acceptance ratios (Figure 2.6) showed an approximate acceptance ratio of 29.4% when

$\xi = 1$, well within the range of the recommendation by Gelman et al. (2004). At $\xi = 1$, the Markov chain was efficient in collecting representative samples and moves actively in the posterior space as shown in the Figure 2.5(b), which is consistent with the previous conclusion in which $\xi = 1$ yielded a converged estimation of statistics of input parameters. Thus, the Markov chain with a sample number of 60,000 and a scaling factor $\xi = 1$ was used in this study, as shown in Figure 2.7.

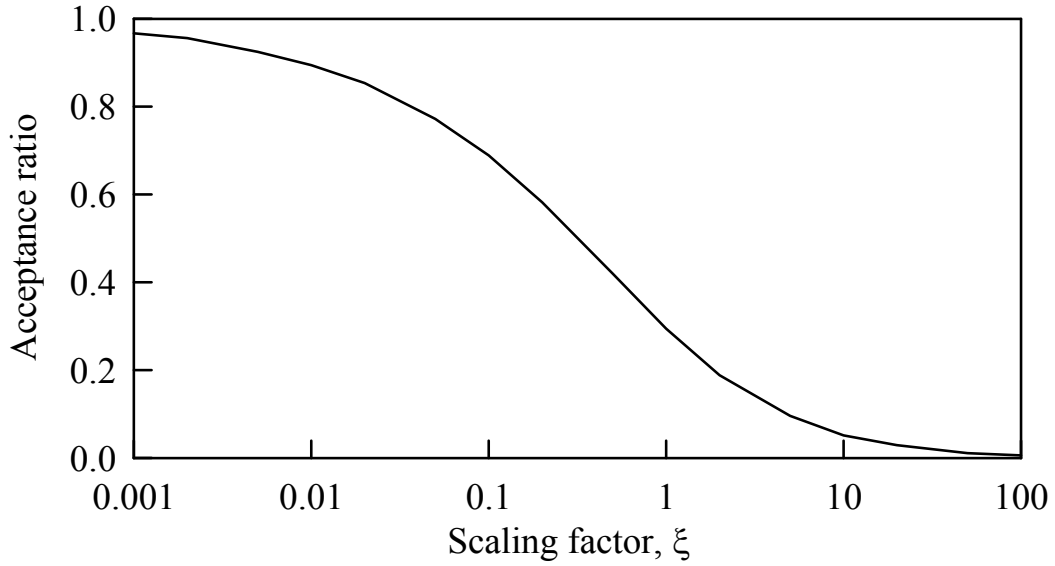

Figure 2.6: Effects of scaling factor ξ on the acceptance ratio of MCMC

Through the resulting histogram of the posterior estimated input parameters, shown in Figure 2.8, the updated mean ϕ was found to be 13.21° (the prior is 21°), and the updated standard deviation was found to be 0.93° (from a prior of 3.15°). These results are consistent with the findings of TGS (2011) in which it was determined that a weakening of shear strength along the slip surface over a long period due to long-term weathering processes was one of the major causes of failure of the slope that had an

observed “average” slip surface of inclination of 15°. The updated parameters also show a reduction in the uncertainty in the friction angle with the new acquired data from field observations.

Figure 2.8 also illustrates a decrease in the mean value of the anchor force T (from 60 ton to 35.29 ton) and a decrease in its standard deviation (from 22.8 ton to 9.81 ton). The decrease of anchor force is consistent with the field observations, indicating that most of anchors underwent pullout failure during slope failure, and that all remaining anchors exhibited significant corrosion on their surfaces. These findings also agree well with the conclusion in the TGS report (2011), which also determined that the corrosion of the anchor system was a primary catalyst and major reason for this slope failure on Freeway No. 3 in Taiwan.

The decrease of the anchor force T is mainly due to the deterioration caused by environmental factors such as the moisture content of the concrete, temperature fluctuation and underground corrosive substances. In a comprehensive seven-year study of bonded anchors, Eligehausen et al. (2006) reported a statistical relationship between the ratio of pullout load after a loading time t over the initial value at t_0. It was determined that after this seven-year period, the strength of the anchors had decreased to approximately 60% of the initial value. In some isolated cases, the strength of the anchors decreased even further, to as little as 30%. The back calculated average ratio of the anchor strength after a long time over the initial design value at t_0 for this failure slope is 59%, which is consistent with the field testing results of 60% as reported by Eligehausen et al. (2006).

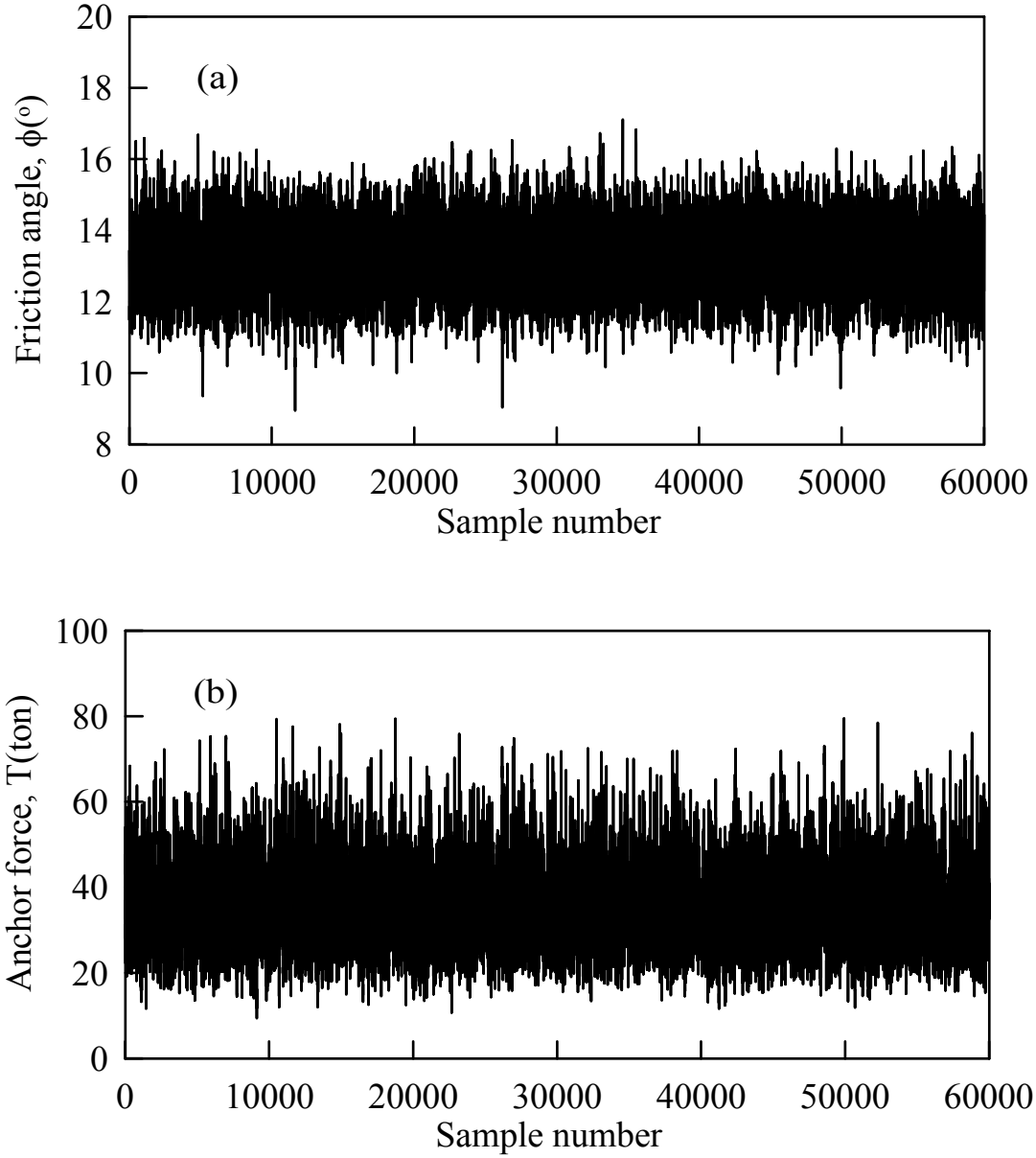

Figure 2.7: Plots of samples for ϕ and T in a Markov chain ($\xi = 1$)

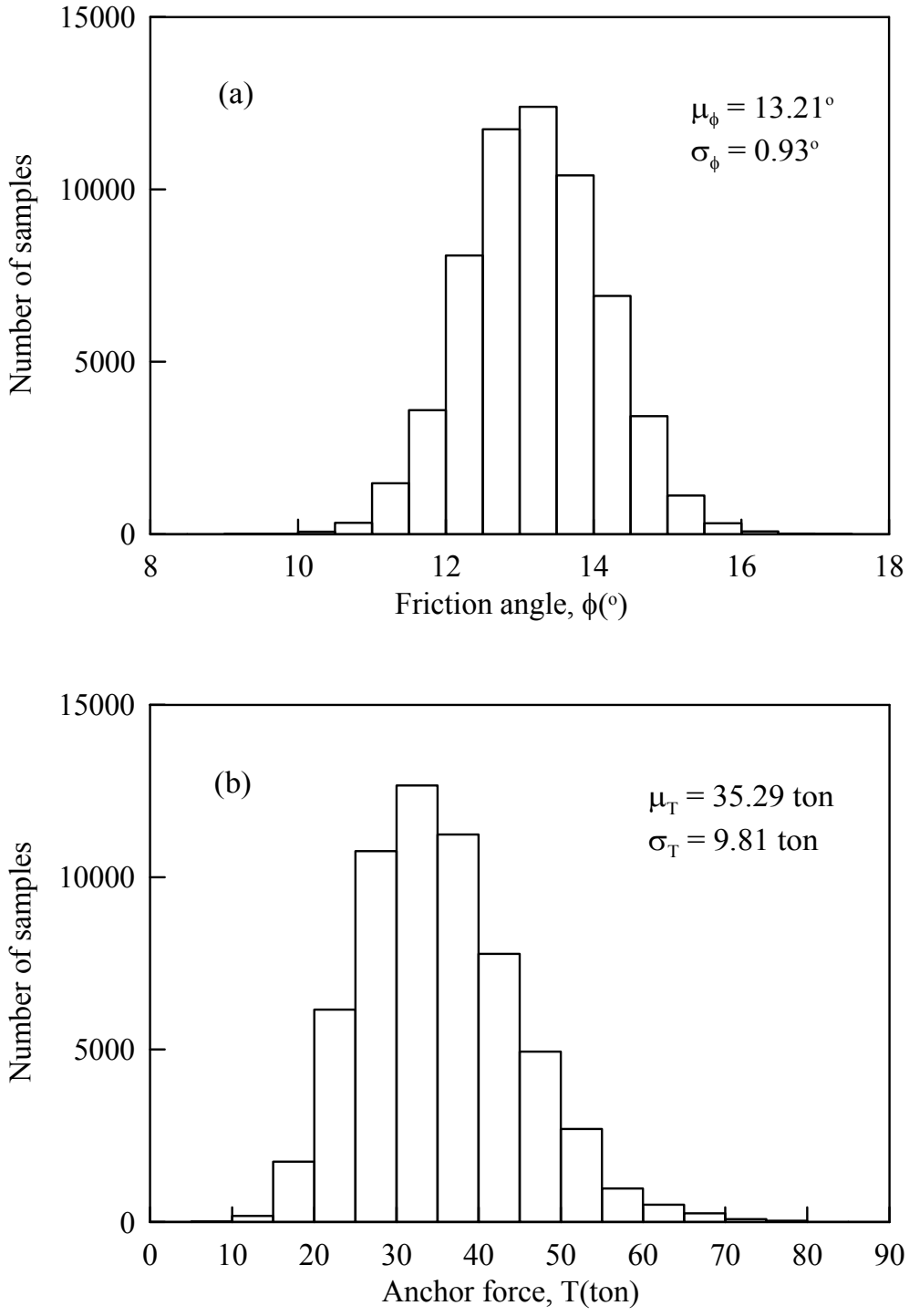

Figure 2.8: Histogram of posterior distribution for ϕ and T obtained from MCMC

Next, a Monte Carlo simulation of 10,000,000 samples was performed to compare the failure probability using prior information and updated parameters. When using the prior distribution, the probability of the slope failure was determined to be 1.77×10^{-4}, which is very low. When using the updated parameters, however, the probability of failure greatly increased, to 0.173, a much higher probability, suggesting the likelihood of slope failure.

Effect of prior distributions

To examine the effect of differently assumed distributions, the Markov Chain Monte Carlo (MCMC)-based back analysis for Freeway No. 3 slope failure was repeated with an assumption of normal prior distribution.

Table 2.6: Comparison of results between the Markov Chain Monte Carlo (MCMC) simulation and the Maximum Likelihood (ML) method

	Mean of ϕ (°)	Std. dev. of ϕ (°)	Mean of T (ton)	Std. dev. of T (ton)
MCMC with lognormal distribution assumption	13.21	0.93	35.29	9.81
MCMC with normal distribution assumption	13.02	1.55	30.62	21.13
ML with lognormal distribution assumption	13.26	1.03	35.02	13.08
ML with normal distribution assumption	12.88	1.49	33.05	20.86

The results of this analysis are shown in Table 2.6. Here, the posterior statistics from the back analysis were most sensitive to the assumed prior distributions, indicating the importance of obtaining high quality prior distributions for the back-analysis of slope failure.

Back Analysis Using Maximum Likelihood Method

Maximum Likelihood Formulation

In addition to the Bayesian approach developed and implemented with MCMC, other methods are available for conducting a back-analysis, as regards to slope failure (e.g. the least squares method, Kalman filter approach, and maximum likelihood (ML) method). In this section, we describe the development of a simplified ML-based formulation in a user-friendly spreadsheet environment to perform this inverse analysis.

In this ML-based formulation, the best estimation of system parameters was obtained by maximizing the likelihood of a hypothesis. The likelihood or posterior estimation is a multiplication of model uncertainty and parameter uncertainty, and is assumed as a multivariate normal distribution (See Appendix A based on Ledesma et al. 1996a). Maximizing the likelihood is equivalent to minimizing the negative log-likelihood function, which is expressed as (Ledesma et al. 1996a&b):

$$S(\boldsymbol{\theta}) = \frac{[g(\boldsymbol{\theta}) + \mu_\varepsilon - Y]^T [g(\boldsymbol{\theta}) + \mu_\varepsilon - Y]}{\sigma_\varepsilon^2} + (\boldsymbol{\theta} - \mu_{\boldsymbol{\theta}})^T \mathbf{C}_{\boldsymbol{\theta}}^{-1} (\boldsymbol{\theta} - \mu_{\boldsymbol{\theta}}) \tag{2.6}$$

where Y is the observed factor of safety, which is equal to 1.0 when slope failure occurs. In this equation, the first term of the right-hand-side represents the error between model prediction and observed value, and the second item represents the difference between the prior information and parameters to be back analyzed. Using Eq. (2.6), the inverse analysis becomes an optimization problem that can be easily resolved using a commonly available spreadsheet (Zhang et al. 2010b).

To solve this problem, the posterior covariance of parameter vector $\boldsymbol{\theta}$ is obtained by linearizing $\boldsymbol{\theta}$ at $\mu_{\boldsymbol{\theta}|Y}$, which is expressed as (Tarantola 2005):

$$\left(\frac{G^T G}{\sigma_\varepsilon^2} + C_{\boldsymbol{\theta}}^{-1} \right)^{-1} \tag{2.7}$$

where G is the partial derivative vector evaluated at the posterior mean value of uncertainty parameters $\mu_{\boldsymbol{\theta}|Y}$:

$$G = \left[\frac{\partial g(\boldsymbol{\theta})}{\partial \boldsymbol{\theta}} \right]_{\boldsymbol{\theta}=\mu_{\boldsymbol{\theta}|Y}} \tag{2.8}$$

This formulation can be implemented within a spreadsheet making it quite handy for use in an engineering application, and requiring much less computational effort. Figure 2.9 shows the layout of one such spreadsheet implemented with the ML-based formulation. The procedure for obtaining the posterior distribution using this approach is described below:

(1) The slope stability model (Eq. 2.1) is implemented in the spreadsheet. The

prior estimation of the mean of input parameters is defined in cells C14:C15, the prior COVs are defined in cells E14:E15, and the model uncertainty parameters are defined in cells G21:H21.

(2) To carry out optimization, the posterior mean of input parameters are obtained by minimizing Eq. (2.6) through the use of Solver function in the spreadsheet. Here, we try to "minimize G25 by changing cells C21:C22." The optimization method can be specified within the Solver function. The resulting posterior mean is shown in cells C21:C22.

(3) The posterior covariance of input parameter vector $\boldsymbol{\theta}$ is estimated with Eq. (2.7), the results of which are shown in cells F32:G33.

Back analysis using maximum likelihood method – Case study

A spreadsheet was developed to conduct the back-analysis of the strength parameter and anchor force of the failed slope on Freeway No. 3 (Figure 2.9). The input parameters were assumed as multivariate normal distributions, the statistics of which are listed in Table 2.2. Here, $FS(\phi, T)$ expressed in Eq. (2.1) is treated as $g(\boldsymbol{\theta})$. The parameters (ϕ and T) are back-calculated using the spreadsheet that implements the procedure described previously. Table 2.6 shows the resulting posterior statistics for both the friction angle and the anchor force. The posterior mean of ϕ is 12.88^{o}, with a standard deviation of 1.49^{o}; and the posterior mean of T is 33.05 ton, with a standard deviation of 20.86 ton. The results agree closely with that obtained with MCMC using the normal prior distribution assumption.

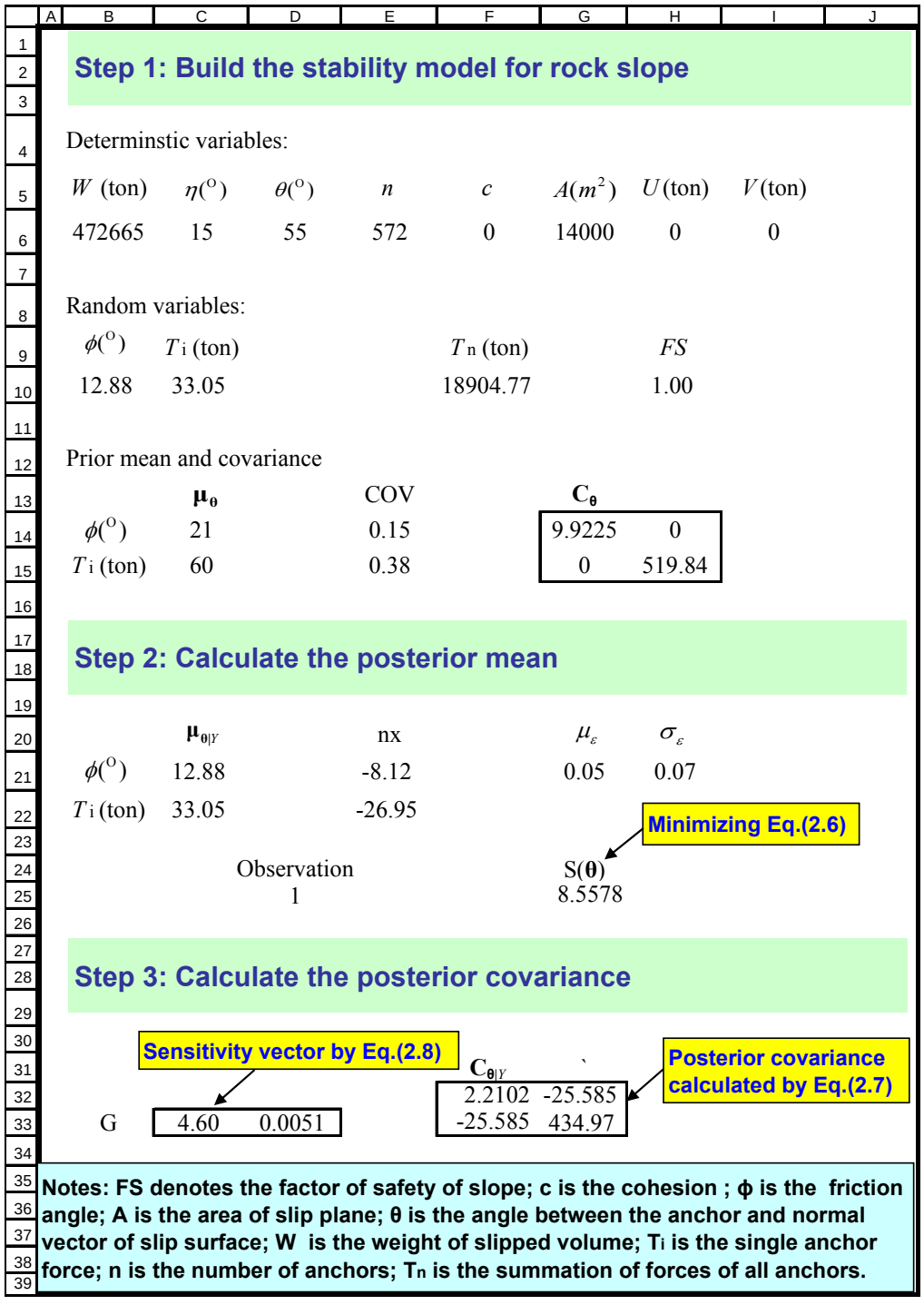

Figure 2.9: Spreadsheet for back analysis of slope with maximum likelihood (ML) method

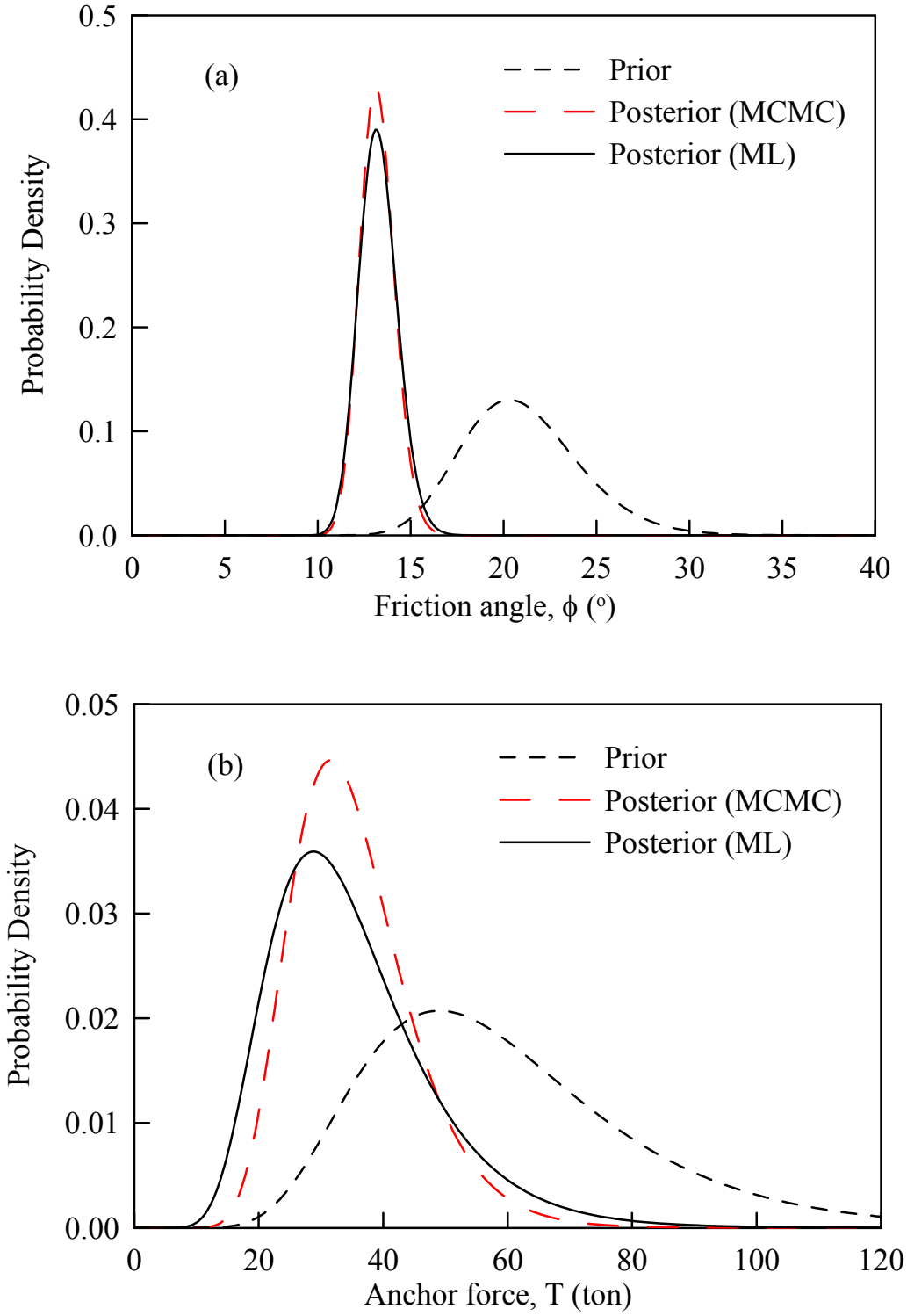

Figure 2.10: Prior and posterior distribution of input parameters assuming lognormal distribution

If the prior distributions of input parameters are assumed as having a lognormal distribution, the prior distribution should first be transformed into normal distributions using a transformation technique (Der Kiureghian 1986; Zhang et al. 2010b). The back analysis results with the lognormal prior distribution assumption are also shown in Table 2.6. In Figure 2.10, we provide a further comparison of the prior and posterior distribution of the input parameters. The results indicate that the uncertainty of input parameters can be reduced through the back analysis *in this case*. The results obtained from the use of this ML-based procedure were consistent with that obtained with the MCMC-based procedure. The minor difference is mainly caused by the simplification of the stability analysis model adopted by the ML-based approach, which involves a linear approximation in the posterior covariance estimation.

In summary, both MCMC-based and ML-based approaches yielded results that were consistent with field observations and the findings of the TGS report (TGS 2011): that the weakening of the shear strength and deterioration of the anchor system were the primary causes for the Freeway No. 3 slope failure. The prior mean of internal friction angle ϕ was 21° and the updated mean based on the probabilistic back analysis is approximately at 13° (Table 2.6), while the average observed slip surface of inclination was approximately 15°. Compared with the MCMC simulation based approach, the ML-based approach is easy to implement in a spreadsheet, requires much less computational effort, and represents a preferred tool for engineering practice. This tool is suitable for use in a post-event failure investigation, and for the evaluation of alternative remedial measures.

Summary

In this chapter, two procedures for the probabilistic back analysis of slope failure were presented using as an example a recent slope failure case on Freeway No. 3 in Taiwan. The internal friction angle and anchor force were determined to be the key parameters in this case. These two parameters are first back-calculated using the Markov Chain Monte Carlo (MCMC) simulation. The second procedure was based on the maximum likelihood (ML) method. Though the two procedures yielded results that were almost identical, and agreed well with field observations, the ML-based procedure required much less computational effort and was easily implemented in a spreadsheet, thus, demonstrating its potential as a practical geotechnical engineering tool.

The enhanced knowledge of the input parameters for the slope system through back analysis was used to elucidate the failure mechanism and yield a more reasonable estimate of the failure probability of the slope. Selecting a proper remediation method is now much more certain with the improved knowledge of input parameters coupling with the reliability-based design approach. In the case study of Freeway No. 3 slope, the back analysis results showed that besides weakening of the shear strength, the deteriorating anchor was a major influence on the slope failure, thus emphasizing the critical importance of maintenance to the anchor system for reducing the possibility of future slope failures.

CHAPTER THREE

PROBABILISTIC BACK ANALYSIS OF BRACED EXCAVATIONS

Introduction

The observational method (Peck 1969) is an important tool in geotechnical engineering. Peck recognized the importance of the observational method, as he "emphasized the need to first compute the various quantities that can be measured in the field and then close the gaps in knowledge on the basis of such measurements" (Wu 2011). In this chapter, this observational method is applied to supported excavation. Here, field observations in a staged excavation are used to update soil parameters, which, in turn, are used to refine the predictions of the wall deflection, ground settlement and damage potential of buildings adjacent to the excavation in the subsequent stages of excavation.

The inverse analysis in the braced excavation is not uncommon. Conventionally, the finite element method (FEM) is utilized to predict the excavation-induced wall and ground responses (e.g., Hashash et al. 2004; Hashash et al. 2006; Tang and Kung 2009; Tang and Kung 2010). In the FEM analysis, the wall deflection, ground settlement and building damage potential are generally predicted and used to check against the acceptance criteria (i.e., Boone 1996). Due to the limited field explorations and

---

*A similar form of this chapter has been submitted at the time of writing: Wang L, Luo Z, Xiao J, Juang CH. Probabilistic inverse analysis of excavation-induced wall and ground responses for assessing damage potential of adjacent buildings.

laboratory tests, the soil parameters used in the FEM analysis may not be representative of field behavior and thus the predicted excavation-induced responses often do not match the field observations. In a project such as braced excavation, the observed wall deflection and ground settlement from the initial excavation stages can be used to update the design soil parameters. The updated soil parameters, which represent the "refined" knowledge of the soil parameters at a given stage, can be used to refine the predictions in the subsequent excavation stages. As the excavation proceeds stage by stage, observations are collected in each stage and the soil parameters can be updated accordingly. Thus, the inverse analysis provides a means to update the prediction of ground responses and assessment of building damage during construction.

Conventional inverse analysis relies on the deterministic approach such as the least squares method, gradient method (Ou and Tang 1994), genetic algorithms (Levasseur et al. 2008), artificial neural networks (Hashash et al. 2006). It should be noted that the deterministic inverse analysis techniques could not deal with explicitly the uncertainty in the soil parameters. It is reported that the uncertainty in soil parameters has a significant influence on the predicted wall and ground responses in braced excavations (Hsiao et al. 2008). In this regard, it is desirable to conduct the probabilistic inverse analysis of a braced excavation. To this end, it is noted that several approaches, including the Kalman filter approach (Eykhoff 1974), the maximum likelihood method (Ledesma et al. 1996b), and the Bayesian method (Honjo et al. 1994; Zhang et al. 2010a), have been shown effective for the probabilistic inverse analysis of some geotechnical problems.

Although FEM can be used in the probabilistic inverse analysis of braced

excavations, it is more efficient, computationally, to combine the observational method with the empirical models such as KJHH (Kung et al. 2007) and KSJH (Schuster et al. 2009). These models, which were developed using well-documented case histories and finite element simulations, can be readily adopted to predict the excavation-induced wall and ground responses and the potential of building damage caused by these responses. To this end, the KJHH model is adopted in this chapter for predicting the excavation-induced wall and ground responses in the probabilistic inverse analysis of braced excavations.

In this chapter, the observational method is combined with the maximum likelihood formulation to update the soil parameters in braced excavations. The prior distributions of soil parameters are estimated based on those reported in the literature and engineering judgment. After the initial excavation stages are conducted, the maximum wall deflection and maximum ground settlement are measured (or observed). Those observations are used to update the soil parameters, and the updated soil parameters are presented as posterior distributions and characterized by their sample statistics. The updated soil parameters are then used to refine the predicted wall and ground responses in the subsequent excavation stages, as well as the building damage potential. This straightforward approach is repeated in a staged excavation, and the soil parameters are updated as the excavation proceeds. Comparing with the predictions using prior distributions, the predictions using the updated soil parameters generally result in an improved accuracy in the prediction of wall and ground responses, which in turn, yield an improved prediction of building damage potential.

Probabilistic Back Analysis Procedure for Braced Excavations

The KJHH model (Kung et al. 2007), a semi-empirical model that was developed based on hundreds of simulations of case histories using finite element method (FEM), is employed herein to predict the maximum wall deflection (δ_{hm}) and maximum ground settlement (δ_{vm}) in a braced excavation in clay. The detailed formulation of the KJHH model is referred to Kung et al. (2007). There are six input parameters in this model, the excavation depth H_e, the excavation width B, the system stiffness $S = EI / \gamma_w h_{avg}^4$, the normalized clay layer thickness ratio $\Sigma H_{clay} / H_{wall}$, the normalized undrained shear strength $s_u / \sigma_v^{'}$, and the normalized initial modulus $E_i / \sigma_v^{'}$. As reported in a sensitivity study by Hsiao et al. (2008), the two uncertain soil parameters ($s_u / \sigma_v^{'}$ and $E_i / \sigma_v^{'}$) are found to be the main factors affecting the responses of a braced excavation. Therefore, the focus of this chapter is to develop procedures for updating $s_u / \sigma_v^{'}$ and $E_i / \sigma_v^{'}$ in a braced excavation using the observed maximum wall and ground responses (or movements in this case). This updating procedure is basically an inverse analysis. However, to account for the uncertainty in the parameters, a probabilistic inverse analysis is presented.

According to Hsiao et al. (2008), all but the two main factors ($s_u / \sigma_v^{'}$ and $E_i / \sigma_v^{'}$) can be treated as constants in the probabilistic inverse analysis. Furthermore, the model biases of the two component models (δ_{hm} and δ_{vm}) of KJHH model were evaluated using case histories by Kung et al. (2007). For the component model that was used to predict

δ_{hm}, the model bias, denoted as $\mathbf{c}_h$ herein, has a mean value of 1.0 and a COV of 0.25; for the component model that was used to predict δ_{vm}, the model bias, denoted as $\mathbf{c}_v$ herein, has a mean value of 1.0 and a COV of 0.34. They considered these model bias factors normally distributed.

In this chapter, the soil parameters are updated using the maximum likelihood principles (Wang et al. 2013). The formulation of the maximum likelihood method for the probabilistic inverse analysis of braced excavations is presented below using the KJHH model as the means for predicting the excavation-induced wall and ground responses.

Symbolically, KJHH model can be expressed as:

$$\mathbf{y} = G(\boldsymbol{\theta}) \tag{3.1}$$

where $\boldsymbol{\theta}$ is the input vector including $s_u / \sigma_v^{'}$ and $E_i / \sigma_v^{'}$ and other fixed parameters, $\mathbf{y}$ is the response vector including both maximum wall deflection and maximum ground settlement at the end of a given excavation stage. The response of the excavation is related to the input parameter vector through the KJHH model denoted as *G*. The correlation between the vector of observations ($\mathbf{Y}$) and the vector of KJHH model predictions ($\mathbf{y}$) can be expressed as follows:

$$\mathbf{Y} = \mathbf{c} \cdot \mathbf{y} = \mathbf{c} \cdot G(\boldsymbol{\theta}) \tag{3.2}$$

where $\boldsymbol{c}$ is a term that represents the model uncertainty. For illustration purpose, let us assume that only one pair of observations (i.e., one observed maximum ground settlement

and one observed maximum wall deflection in the same excavation stage) is available for back analysis (or inverse analysis) of soil parameters. Note that the model uncertainty of the KJHH model is reflected through the use of bias factors in multiplication form (as in Eq. 3.2) with a mean vector of $\mu_{\mathbf{c}} = [\mu_{\mathbf{c}_h}, \mu_{\mathbf{c}_v}]$ and a covariance matrix of:

$$\sigma_{\mathbf{c}}^2 = \begin{bmatrix} \sigma_{\mathbf{c}_h}^2 & \sigma_{\mathbf{c}_{hv}}^2 \\ \sigma_{\mathbf{c}_{vh}}^2 & \sigma_{\mathbf{c}_v}^2 \end{bmatrix} \tag{3.3}$$

where $\sigma_{\mathbf{c}_{hv}}^2 = \sigma_{\mathbf{c}_{vh}}^2 = \rho \cdot \sigma_{\mathbf{c}_h} \cdot \sigma_{\mathbf{c}_v}$ and ρ is the correlation coefficient between two model bias factors $\mathbf{c}_h$ and $\mathbf{c}_v$ (Juang et al. 2013). In the common maximum likelihood formulation, the model bias of the observation model is often expressed in "addition" form (Tarantola 2005). With the mean vector of model bias, $\mu_{\mathbf{c}} = [1, 1]$, Eq. (3.2) can be converted into an addition form as follows (Wang et al. 2013):

$$\mathbf{Y} = \mathbf{c} \cdot G(\boldsymbol{\theta}) = \mu_{\mathbf{c}} \cdot G(\boldsymbol{\theta}) + \varepsilon = \mu_{\mathbf{c}} \cdot \mathbf{y} + \varepsilon = \mathbf{y} + \varepsilon \tag{3.4}$$

where ε is the residual error vector and is assumed to follow a multivariate normal distribution $\varepsilon \sim N(0, \mathbf{C}_\varepsilon)$. The covariance $\mathbf{C}_\varepsilon$ depends on both the covariance of model bias factor vector $\sigma_{\mathbf{c}}$ and the input parameter vector $\boldsymbol{\theta}$, which can be expressed as:

$$\mathbf{C}_\varepsilon = \begin{bmatrix} (\sigma_{\mathbf{c}_h} \cdot G_h(\boldsymbol{\theta}))^2 & (\sigma_{\mathbf{c}_{hv}} \cdot G_{hv}(\boldsymbol{\theta}))^2 \\ (\sigma_{\mathbf{c}_{vh}} \cdot G_{vh}(\boldsymbol{\theta}))^2 & (\sigma_{\mathbf{c}_v} \cdot G_v(\boldsymbol{\theta}))^2 \end{bmatrix} \tag{3.5}$$

where $G_{hv}^2(\boldsymbol{\theta}) = G_{vh}^2(\boldsymbol{\theta}) = G_v(\boldsymbol{\theta}) \cdot G_h(\boldsymbol{\theta})$ and where $G_h(\boldsymbol{\theta})$ and $G_v(\boldsymbol{\theta})$ are the predicted δ_{hm}

and the predicted δ_{vm}, respectively.

It should be noted that the aforementioned model uncertainty in the formulation of Eq. (3.5) is derived for the scenario when only one pair of observations (namely one maximum ground settlement and one maximum wall deflection) at a given excavation stage is adopted. If the observations from multiple excavation stages (say, *n* stages with totally *N=2n* observations) are available, the covariance $\mathbf{C}_{\varepsilon}$ can be transformed into a $N \times N$ covariance matrix similar to one expressed in Eq. (3.5). For instance, when observations of the i^{th} and the j^{th} stages are available, $\mathbf{C}_{\varepsilon}$ can be expanded into:

$$\mathbf{C}_{\varepsilon} = \begin{bmatrix} (\sigma_{\mathbf{c}_h} \cdot G_{hi}(\boldsymbol{\theta}))^2 & (\sigma_{\mathbf{c}_{hv}} \cdot G_{hvi}(\boldsymbol{\theta}))^2 & 0 & 0 \\ (\sigma_{\mathbf{c}_{vh}} \cdot G_{vhi}(\boldsymbol{\theta}))^2 & (\sigma_{\mathbf{c}_v} \cdot G_{vi}(\boldsymbol{\theta}))^2 & 0 & 0 \\ 0 & 0 & (\sigma_{\mathbf{c}_h} \cdot G_{hj}(\boldsymbol{\theta}))^2 & (\sigma_{\mathbf{c}_{hv}} \cdot G_{hvj}(\boldsymbol{\theta}))^2 \\ 0 & 0 & (\sigma_{\mathbf{c}_{vh}} \cdot G_{vhj}(\boldsymbol{\theta}))^2 & (\sigma_{\mathbf{c}_v} \cdot G_{vj}(\boldsymbol{\theta}))^2 \end{bmatrix} \tag{3.6}$$

where $G_{hi}(\boldsymbol{\theta})$ and $G_{vi}(\boldsymbol{\theta})$ denote the predicted maximum wall deflection and ground settlement at i^{th} stage similar to Eq. (3.5). It should be noted that the correlation of model uncertainty exists only in the predicted wall deflection and ground settlement at the same stage, while observations at different stages are assumed independent from each other, and the model uncertainty of the observation model for various stages are assumed to be uncorrelated (Park et al. 2010).

Assuming that the soil parameters follow a multivariate normal distribution, with *M* input parameters, the probability density function can be expressed as (Ang and Tang 2007; Wang et al. 2010):

$$f(\boldsymbol{\theta}) = \frac{1}{\sqrt{(2\pi)^M \mid \mathbf{C}_{\boldsymbol{\theta}} \mid)}} \exp[-\frac{1}{2}(\boldsymbol{\theta} - \mu_{\boldsymbol{\theta}})^T \mathbf{C}_{\boldsymbol{\theta}}^{-1}(\boldsymbol{\theta} - \mu_{\boldsymbol{\theta}})] \tag{3.7}$$

where $\mu_{\boldsymbol{\theta}}$ is the prior mean vector of input parameters and $\mathbf{C}_{\boldsymbol{\theta}}$ is the prior covariance matrix of the input parameters.

As in Eq. (3.4), the residual error ε is assume to follow a multivariate normal distribution with a zero mean and a covariance matrix of $\mathbf{C}_{\varepsilon}$. Thus, the probability density function of the actual system responses $\mathbf{y} = G(\boldsymbol{\theta})$, given the observed responses ($\mathbf{Y}$), can be described as follows (Ledesma et al. 1996b):

$$f(\mathbf{y} \mid \mathbf{Y}) = \frac{1}{\sqrt{(2\pi)^N \mid \mathbf{C}_{\varepsilon} \mid)}} \exp[-\frac{1}{2}(G(\boldsymbol{\theta}) - \mathbf{Y})^T \mathbf{C}_{\varepsilon}^{-1}(G(\boldsymbol{\theta}) - \mathbf{Y})] \tag{3.8}$$

where N is the number of observations and $\mathbf{C}_{\varepsilon}$ is $N \times N$ covariance matrix of model uncertainty. The likelihood is proportional to the product of the joint probability density of actual system responses given the observations (Eq. 3.8) and the prior distribution (Eq. 3.7) as follows (Ledesma et al. 1996a):

$$L(\boldsymbol{\theta}) \propto f(\mathbf{y} \mid \mathbf{Y}) \cdot f(\boldsymbol{\theta}) \tag{3.9}$$

In the maximum likelihood approach, the parameters are estimated by maximizing the likelihood of a hypothesis. The posterior mean of $\boldsymbol{\theta}$, denoted as $\mu_{\boldsymbol{\theta}|\mathbf{Y}}$, is an optimal value which maximizes Eq. (3.9). For computational efficiency, the logarithm of the likelihood function is selected as the objective function. Thus, maximizing the likelihood (Eq. 3.9)

is equivalent to minimizing the negative log-likelihood function, defined as $S(\boldsymbol{\theta}) = -2\ln L(\boldsymbol{\theta})$. This new likelihood function $S(\boldsymbol{\theta})$ can be simplified as (Ledesma et al. 1996a; Zhang et al. 2010b; Wang et al. 2013):

$$S(\boldsymbol{\theta}) = (G(\boldsymbol{\theta}) - \mathbf{Y})^T \mathbf{C}_{\varepsilon}^{-1} (G(\boldsymbol{\theta}) - \mathbf{Y}) + (\boldsymbol{\theta} - \mu_{\boldsymbol{\theta}})^T \mathbf{C}_{\boldsymbol{\theta}}^{-1} (\boldsymbol{\theta} - \mu_{\boldsymbol{\theta}}) \tag{3.10}$$

The posterior mean $\mu_{\boldsymbol{\theta}|\mathbf{Y}}$ is obtained by minimizing $S(\boldsymbol{\theta})$. Then, the covariance of the posterior distribution can be calculated as follows (Tarantola 2005):

$$\mathbf{C}_{\mathbf{p}} = \left(\mathbf{H}^T \mathbf{C}_{\varepsilon}^{-1} \mathbf{H} + \mathbf{C}_{\boldsymbol{\theta}}^{-1} \right)^{-1} \tag{3.11}$$

where $\mathbf{H}$ is defined as the partial derivative vector evaluated at the posterior mean $\mu_{\boldsymbol{\theta}|\mathbf{Y}}$:

$$\mathbf{H} = \left[\frac{\partial G(\boldsymbol{\theta})}{\partial \boldsymbol{\theta}} \right]_{\boldsymbol{\theta} = \mu_{\boldsymbol{\theta}|\mathbf{Y}}} \tag{3.12}$$

The above procedure is for updating soil parameters with both observations of the maximum ground settlement and the maximum wall deflection. If only one type of observation is available, the above framework can be easily adapted. This formulation can be implemented in a spreadsheet following the similar procedures in Chapter Two.

Case Study: TNEC Excavation Case

To demonstrate the maximum likelihood-based formulation for the probabilistic inverse analysis, a well-documented excavation case history, the Taipei National

Enterprise Center (TNEC), is analyzed here. TNEC excavation site is located in the Taipei Basin, and the seven-staged excavation is mainly conducted in deposits of soft to medium clay (see Figure 3.1). The well-documented field observations of ground surface settlement and wall deflection of TNEC case (Ou et al. 1998) is well suited for the validation of the proposed approach.

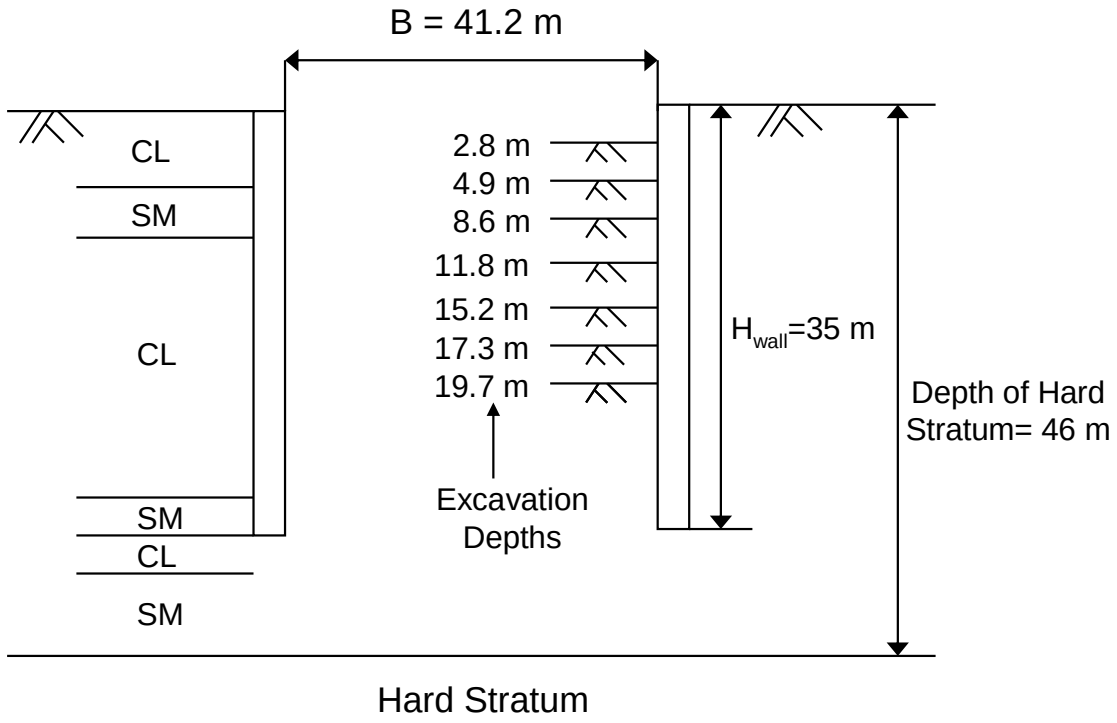

Figure 3.1: Soil profile and excavation depths of TNEC (adapted from Kung et al. 2007)

The TNEC excavation was carried out using the top-down construction method with a maximum depth of 19.7 m. A diaphragm wall with 35 m in depth and 0.9 m in thickness was used as the retaining wall. The details of excavation can be found in Ou et al. (1998). Figure 3.1 shows the excavation depths for seven stages and the corresponding soil profile. The site of TNEC is mainly a clay-dominated site (Kung et al. 2007). It

should be noted that $s_u / \sigma_v^{'}$ and $E_i / \sigma_v^{'}$ of the two clay layers in Figure 3.1 are approximately the same, and the maximum wall and ground responses in this excavation are mainly influenced by $s_u / \sigma_v^{'}$ and $E_i / \sigma_v^{'}$ of the clay layers. As aforementioned, the soil parameters of the clay layers ($s_u / \sigma_v^{'}$ and $E_i / \sigma_v^{'}$) are the dominating parameters that will be updated with field observations. The input parameters of KJHH model of the TNEC case for each stage are listed in Table 3.1.

Table 3.1: Excavation depths and system stiffness of TNEC case history (adapted from Hsiao et al. 2008)

Factor	Excavation sequence (Stage No.)				
	3	4	5	6	7
Depth, H_e (m)	8.6	11.8	15.2	17.3	19.7
System stiffness, $EI/\gamma_w h_{avg}^4$	1023	966	1109	1115	1294

Note: Other deterministic factors required for computing maximum wall deflection and ground surface settlement using KJHH model include: excavation width B = 41.2 m, normalized clay-layer thickness $\sum H_{clay} / H_{wall}$ = 0.87.

Updating using both observed wall deflection and ground settlement

The prior distribution of the soil parameters must be estimated before the soil parameters can be updated. Based on the typical range of the two soil parameters $s_u / \sigma_v^{'}$ and $E_i / \sigma_v^{'}$ reported by Kung (2003), four different prior distributions of soil parameters are assumed and summarized in Table 3.2. For illustration purpose, Prior distribution 1 is adopted herein as the prior distribution of soil parameters vector ($s_u / \sigma_v^{'}$ and $E_i / \sigma_v^{'}$).

The parametric study using various assumed prior distributions will be presented later. Since there is no information regarding the correlation between two model bias factors, the correlation coefficient (ρ) is assumed to be zero for simplicity. Nevertheless, the effects of ρ on the updated results are investigated later. It should be mentioned that the field observations from Stage 1 and Stage 2 are not used in the updating process because the wall deformation shape at these early stages is of cantilever type, which is not compatible with the shape of bulging movement in latter stages (Kung et al. 2007). Thus, updating with the observations from Stages 1 and 2 is fruitless. Fortunately, the wall and ground responses in first two stages under normal workmanship are generally very small, and thus, the wall and ground movements at these early are negligible in the updating process (Hsiao et al. 2008; Juang et al. 2013).

Table 3.2: Statistics of four prior distributions used in the probabilistic back analysis process of TNEC case history (adapted from Juang et al. 2013)

Parameter	$s_u / \sigma_v^{'}$		$E_i / \sigma_v^{'}$	
	Mean	COV*	Mean	COV*
Prior distribution 1	0.25	0.16	500	0.16
Prior distribution 2	0.31	0.16	650	0.16
Prior distribution 3	0.27	0.16	550	0.16
Prior distribution 4	0.35	0.16	750	0.16

*COV suggested by Hsiao et al. (2008) for Taipei clays. The effects of various assumed COVs are examined separately.

As shown in Figure 3.2, the predicted maximum ground settlement at excavation depth of 8.6 m (Stage 3) using the mean of soil parameters (Prior distribution 1) is 47.5 mm prior to Stage 3 of excavation, which is inconsistent with the observed settlement in

field at excavation depth of 8.6 m (18.2 mm). The comparisons of the predicted and observed maximum settlement and wall deflection at different excavation depths (corresponding to different stages in Table 3.1) prior to Stage 3 are shown with "square" notations in Figure 3.2. It is obvious that the predicted responses differ significantly from the observations. After Stage 3 is completed, the soil parameters are updated using the observed wall and ground responses and the developed procedure. With the updated soil parameters in Stage 3, the maximum wall and ground responses in subsequent stages are predicted and compared with field observations. The results are presented with "circle" symbols in Figure 3.2 and denoted as the predictions made "Prior to Stage 4". With the updated soil parameters, the predicted responses match better with the observations (as evidenced by the data points being closer to the perfectly matched line). After Stage 4 of excavation is completed, the observations (settlement and wall deflection) at both Stage 3 and Stage 4 are employed to update further the soil parameters as well as the predictions of the wall and ground responses in subsequent stages. This process continues until the stage prior to the final stage (Stage 7).

As the staged excavation proceeds, more observations from the previous stages become available. In this study, those observations (in terms of maximum wall deflection and ground settlement) of all the previous stages are used to update the soil parameters using the maximum likelihood method. As shown in Figure 3.2, at the completion of Stage 6, the predicted wall deflection and ground settlement prior to the final stage agree well with the observations at the completion of final stage (Stage 7). It is also observed from Figure 3.2 that the predicted wall deflection matches the field observation better

than the settlement does; this is consistent with findings by other previous investigators: the wall deflection is generally easier to predict accurately; the prediction of settlement is, however, more difficult (Finno 2007).

The final excavation stage (Stage 7 with a final excavation depth of 19.7 m) is considered the most critical in the serviceability assessment of adjacent buildings. Figure 3.3 shows the predicted maximum settlement and wall deflection of the last stage using the updated soil parameters at various excavation stages. In Figure 3.3, the predicted mean of wall deflection and ground settlement at the completion of the last stage of excavation is refined as the excavation proceeds. It indicates that as the soil parameters are updated with more and more quality observations, the predicted wall and ground responses can be significantly improved accordingly.

Updating using observed wall deflection or ground settlement

When the observation data is limited (for example, in many case histories, only the observed wall deflection is available), the updating of soil parameters may also be realized using only one type of observation (either wall deflection or ground settlement). For demonstration purpose, Prior distribution 1 is selected as the prior distribution of soil parameters. The aforementioned procedure for updating soil parameters using the maximum likelihood formulation is repeated using the observed wall deflection (or ground settlement) alone. With the updated soil parameters at various excavation stages, the predicted wall and ground responses at the final excavation stage are obtained and plotted in Figure 3.4. The updated predictions shown in Figure 3.3 are also plotted in

Figure 3.4 for comparison. The results show the proposed framework is also effective and efficient even when the soil parameters are updated with only one type of response observation (either maximum settlement or maximum wall deflection).

It is also useful to examine the distributions of the predicted wall and ground responses using the updated soil parameters. The probability distributions of the updated ground settlement and wall deflection predictions, prior to the last stage, using three updating schemes are shown in Figure 3.5. The results show that the means of the updated predictions are quite consistent with the observations. The variation in the predicted wall and ground responses is the smallest when both types of observations are used in the updating. In addition, the variation of the predicted wall and ground responses using only settlement observation is smaller than that using only wall deflection. This is mainly because the error vector of the observational model for ground settlement is smaller than that for wall deflection. It should be noted that in the traditional back analysis of braced excavations, which tries to match "the prediction" to be exact as "observation," the predicted ground settlement and wall deflection are a constant. However, the geotechnical inverse analysis involves model uncertainty as well as the uncertainty of soil parameters. Due to those uncertainties, it is more rational to interpret the updated soil parameters as well as the predicted wall and ground responses as a random variable rather than a single fixed value. The developed procedure for back analysis using the maximum likelihood method in this study contributes to the probabilistic characterization of soil parameters and the fully probabilistic analysis of serviceability assessment in a braced excavation.

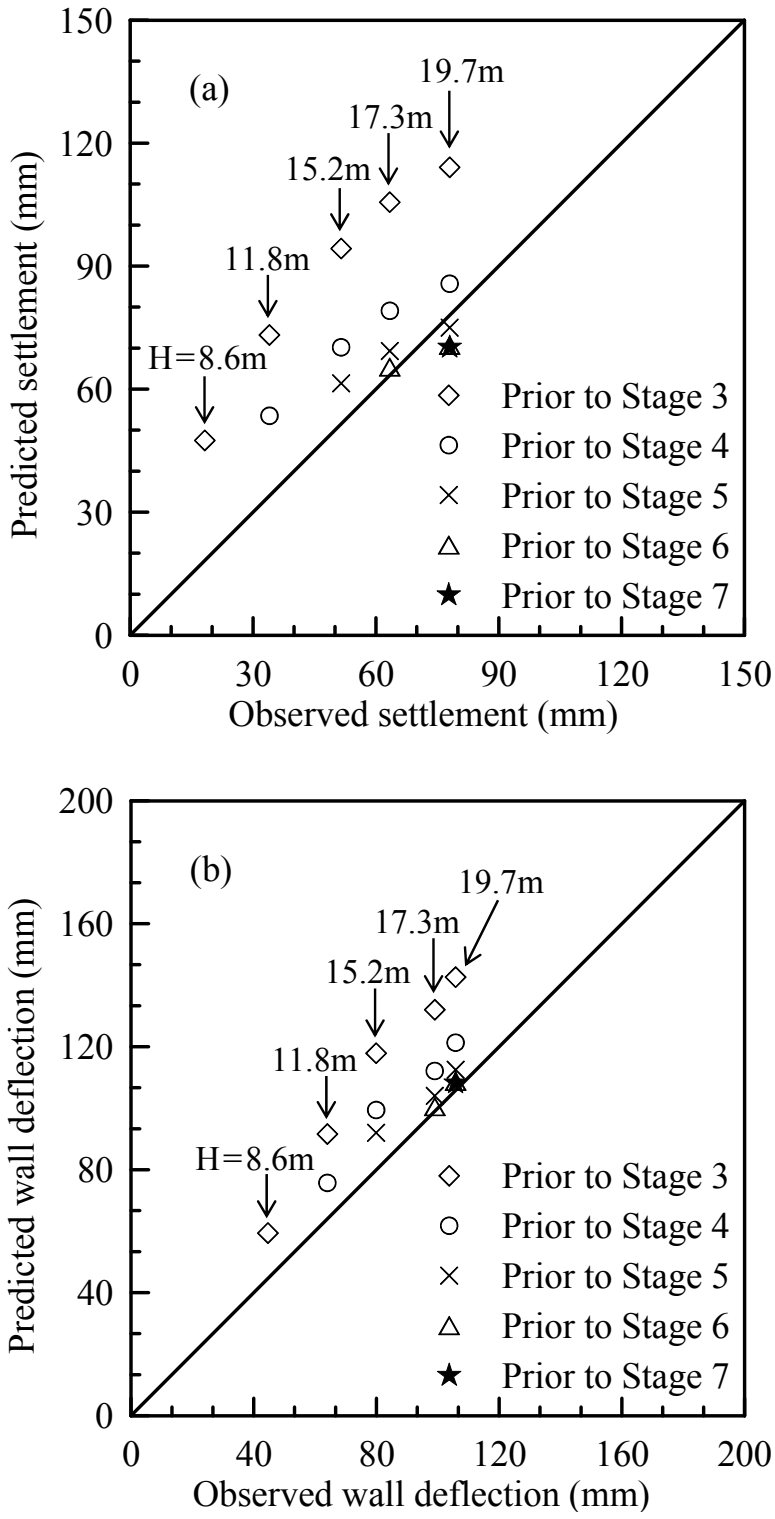

Figure 3.2: Maximum settlement and wall deflection predictions prior to different stages using Prior distribution 1

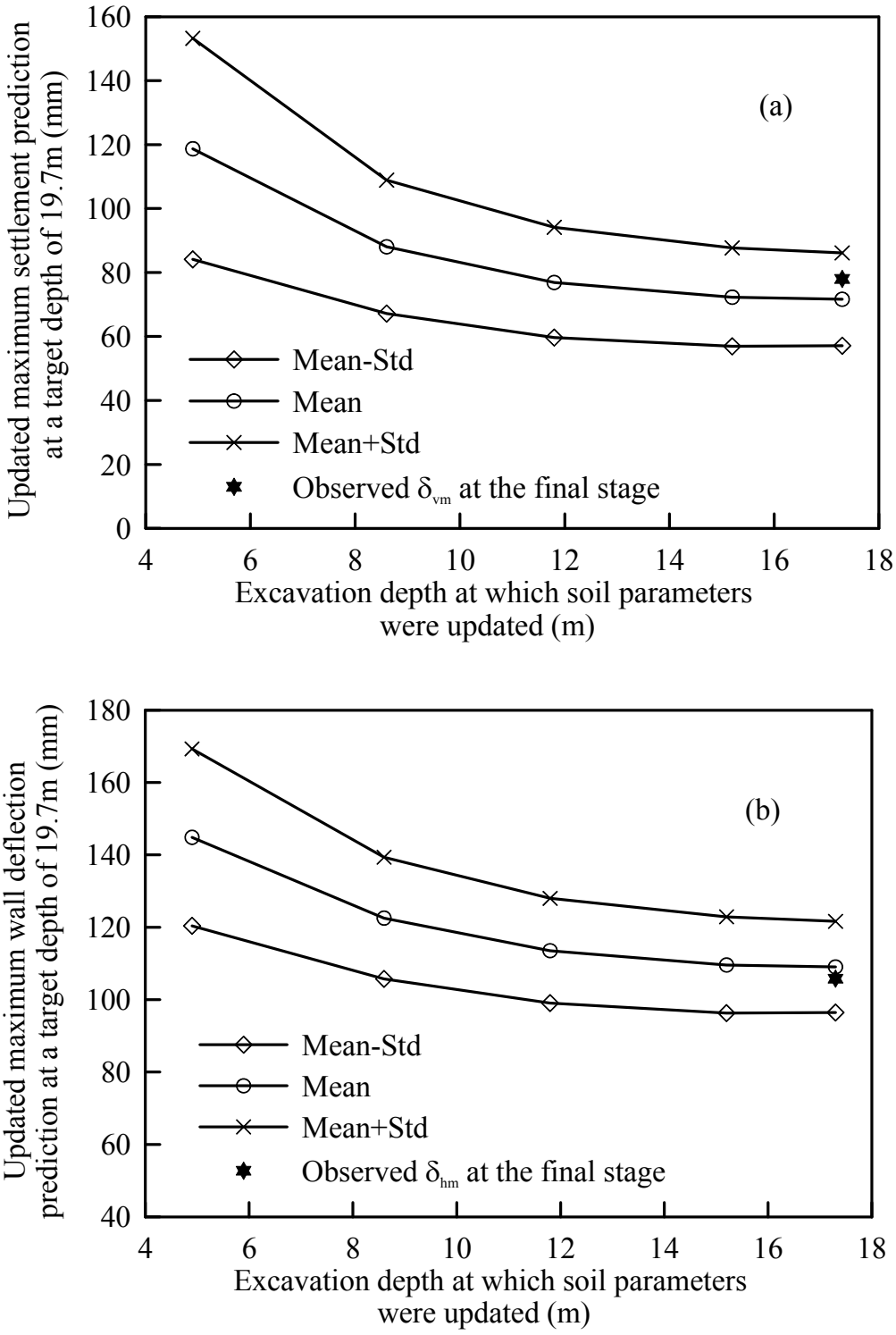

Figure 3.3: Updated mean value and one standard deviation bounds of settlement and wall deflection prior to different stages using Prior distribution 1

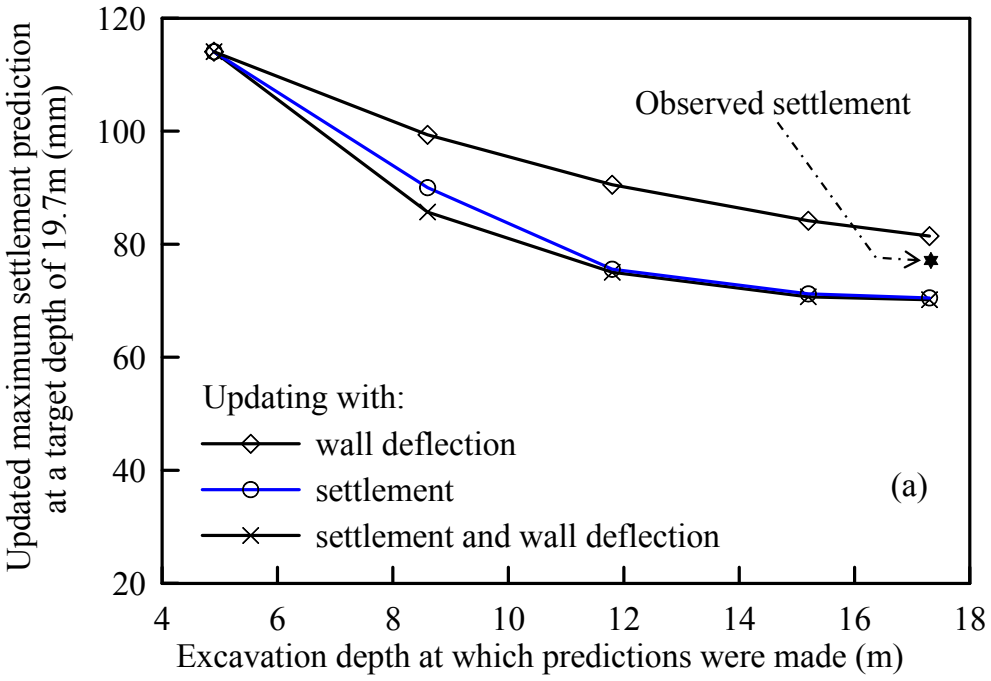

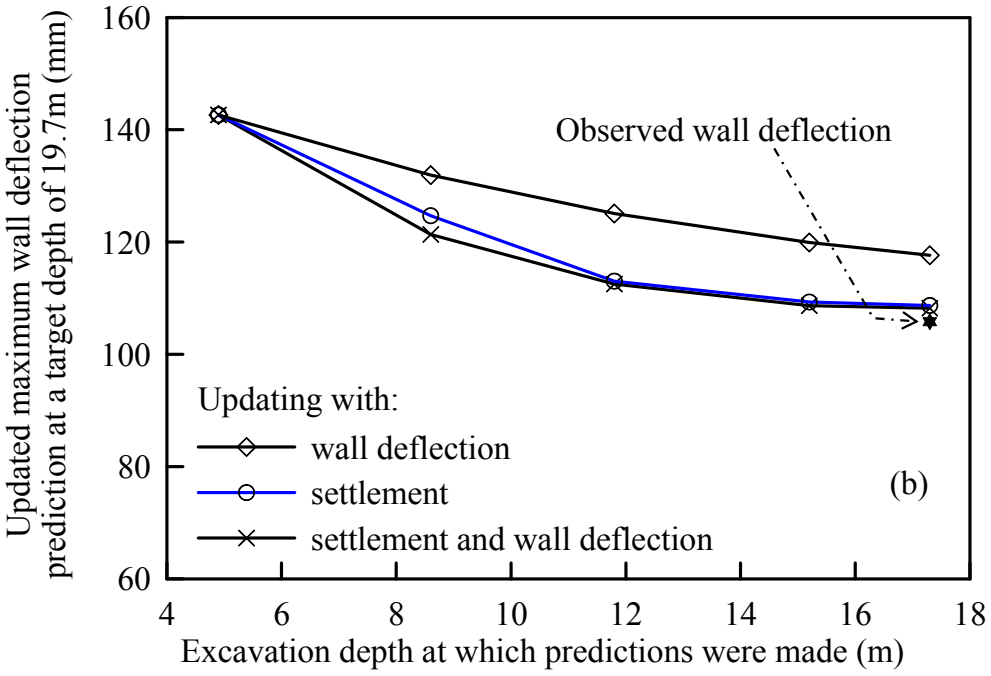

Figure 3.4: Comparisons of updated predictions with three updating schemes (using Prior distribution 1)

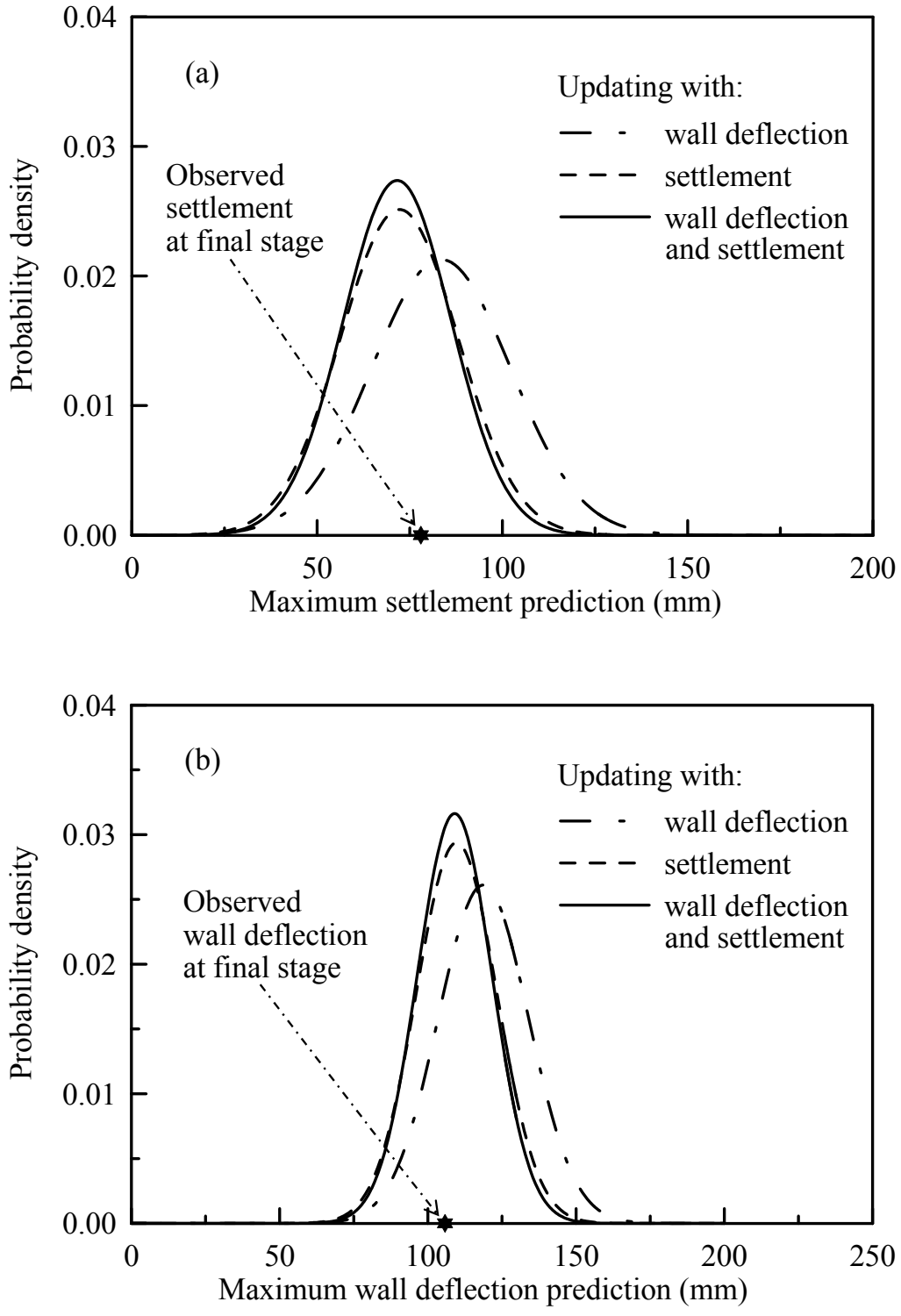

Figure 3.5: Distributions of predictions prior to final stage of excavation (using Prior distribution 1)

Further Sensitivity Analyses and Discussions

Effect of prior distribution on the updating results

The posterior distribution depends on both model and prior distribution, as shown in Eq. (3.10). Due to the insufficient field investigations and potential disturbance in sampling, the estimation of the prior soil parameters could vary significantly. In this regard, it is necessary to investigate the effects of estimated or assumed prior distribution on the updating results. Thus, in addition to Prior distribution 1 (Table 3.2), three other prior distributions are assumed based on the test results of Taipei clay (Kung 2003), as shown in Table 3.2. The four assumed prior distributions cover the possible variation for the two soil parameters ($s_u / \sigma_v^{'}$ and $E_i / \sigma_v^{'}$) for the TNEC case (Juang et al. 2013). The COV of the four distributions is set to be 0.16 as suggested by Hsiao et al. (2008), although other values may also be possible. The effects of the magnitude of COV will be examined later.

The effects of prior distributions on the updated wall and ground responses are studied using two types of observations (both wall deflection and settlement). Following the aforementioned procedure, the updated mean values of $s_u / \sigma_v^{'}$ and $E_i / \sigma_v^{'}$ prior to various excavation depths are shown in Figure 3.6. As shown in Figure 3.6(a), the updated mean values of $s_u / \sigma_v^{'}$ prior to last stage are almost identical no matter what prior distribution is assumed. The updated means of $E_i / \sigma_v^{'}$ also tend to converge as the excavation proceeds, regardless of the assumed prior distributions.

Figure 3.7 shows the updated COV for $s_u / \sigma_v^{'}$ and $E_i / \sigma_v^{'}$ with excavation depths. It is observed that the COV decreases as the excavation proceeds in this example. It indicates that the newly gained "information" from field observations can reduce the estimated variation of soil parameters. Although the variation of soil parameters is reduced most for Prior distribution 1, the COV for all four assumed prior distributions decreases after updating, from 16% to about 10%.

The effect of different assumed COV on the updated results is plotted in Figure 3.8. The distribution 1 is used for illustration and additional COV values of 0.10 and 0.30 are assumed to illustrate the possible overestimation and underestimation of the COV values for $s_u / \sigma_v^{'}$ and $E_i / \sigma_v^{'}$. It can be found that the updated COV value of parameters decreases stage by stage with the updating process regardless which prior COV value is assumed. When the prior estimation of COV is at higher end (30% in this example), the effects of reducing the parameter uncertainty is more effective, and the COV decreases to approximately 12%. When the prior estimation of COV is already quite small (10%), the COV can still be reduced (to approximately 6% in this case).

Figure 3.9 further compares the probability distribution of $s_u / \sigma_v^{'}$ and $E_i / \sigma_v^{'}$ before and after the updating process. The uncertainties of soil parameters are reduced significantly through the soil parameters that are updated with field observations. In the example studied, the COV of $s_u / \sigma_v^{'}$ decreases from 0.16 to approximately 0.08 and the COV of $E_i / \sigma_v^{'}$ decreases from 0.16 to approximately 0.09.

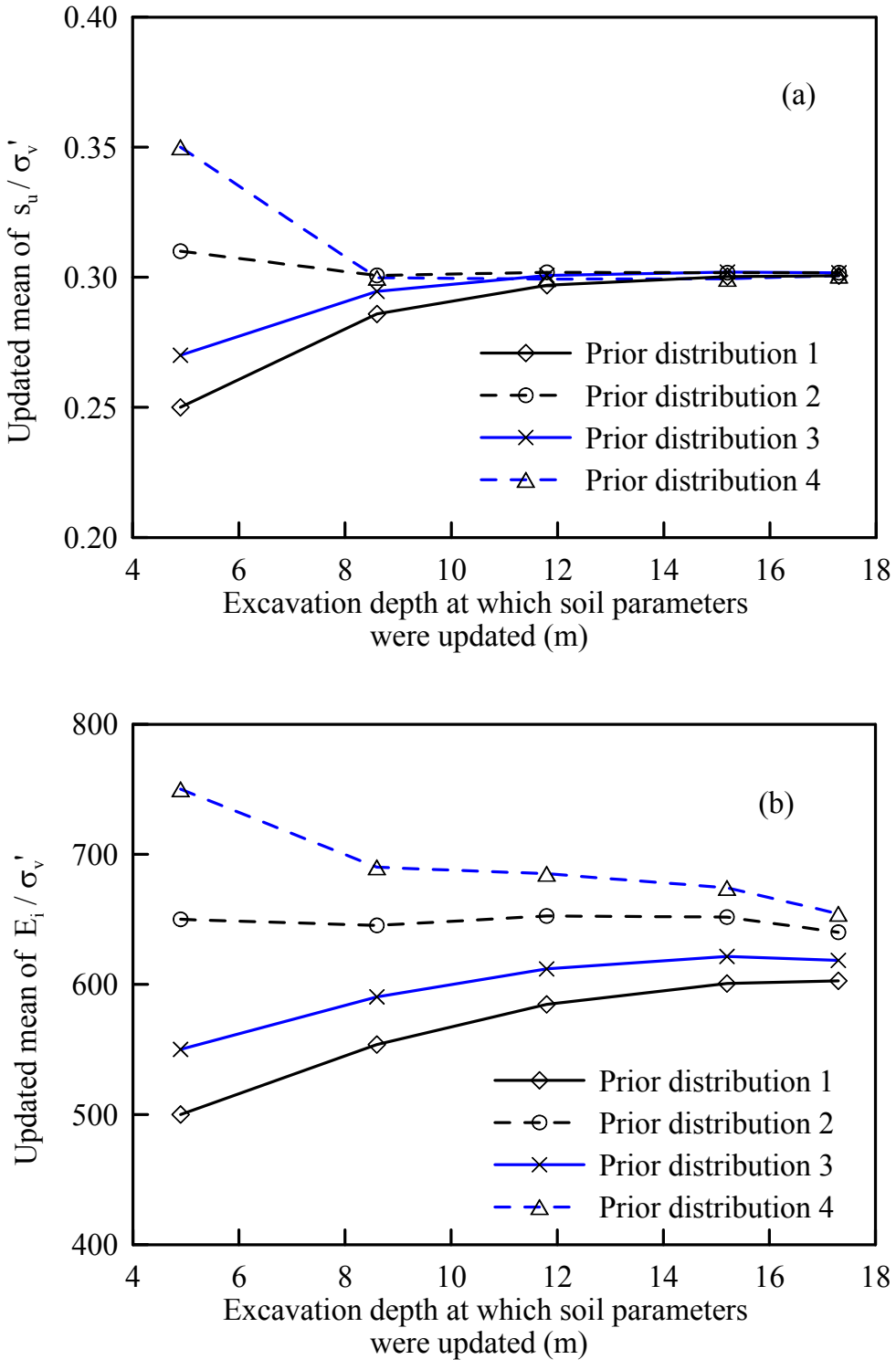

Figure 3.6: Comparisons of updated mean of soil parameters prior to different stages with various prior distributions

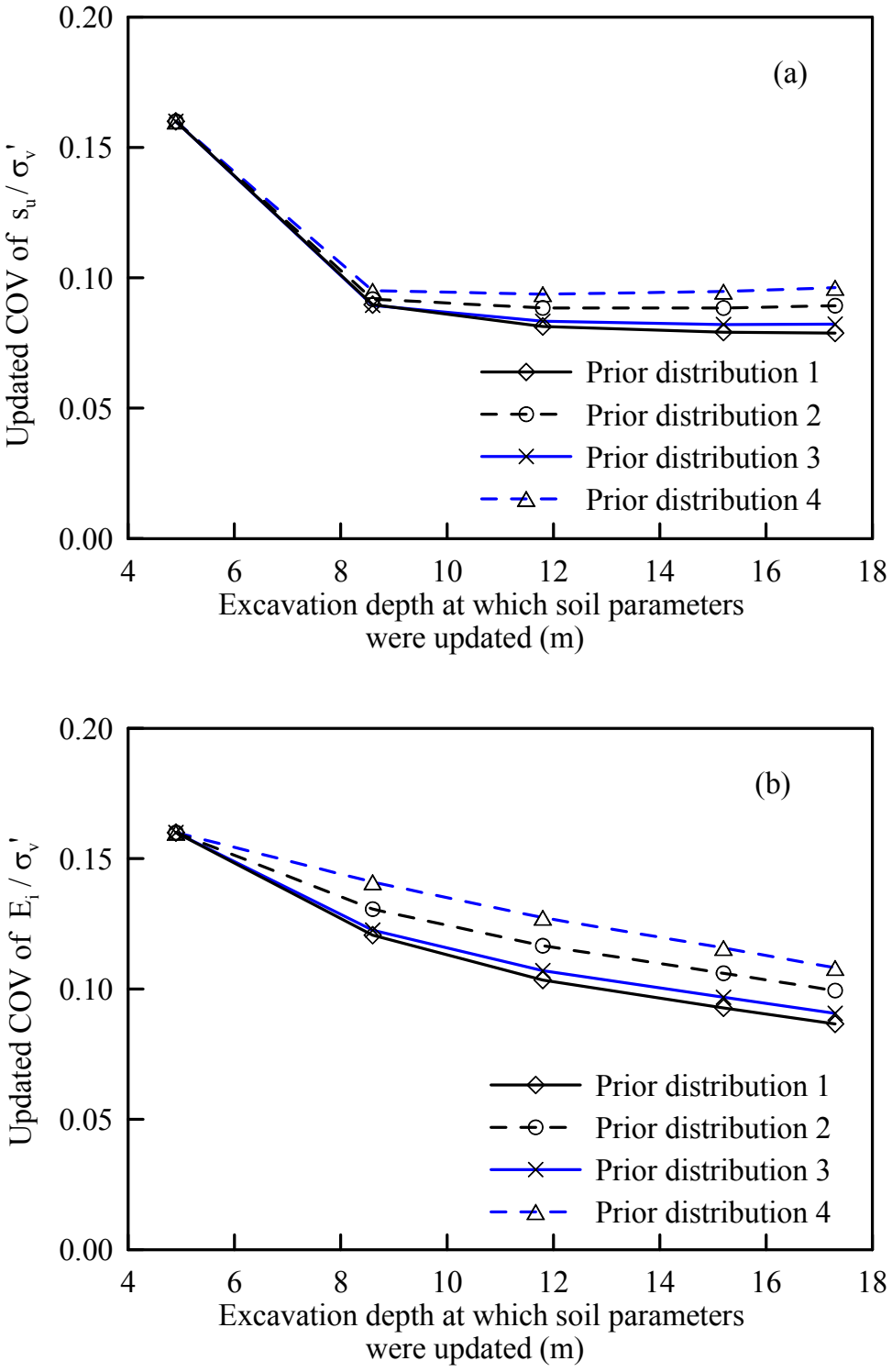

Figure 3.7: Comparisons of updated COV of soil parameters prior to different stages with various prior distributions

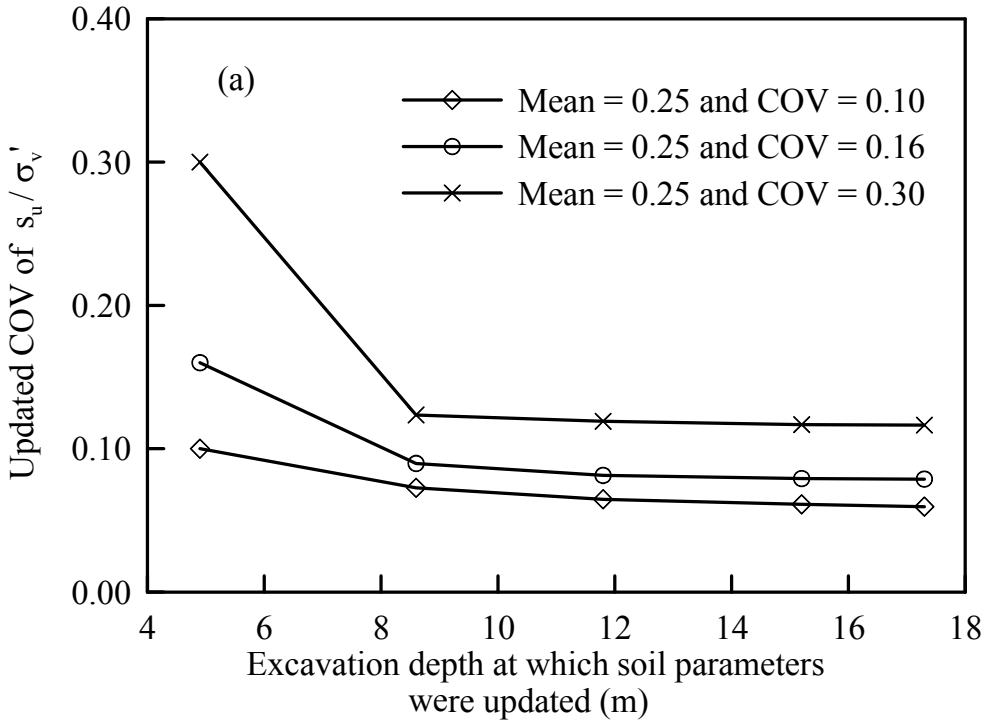

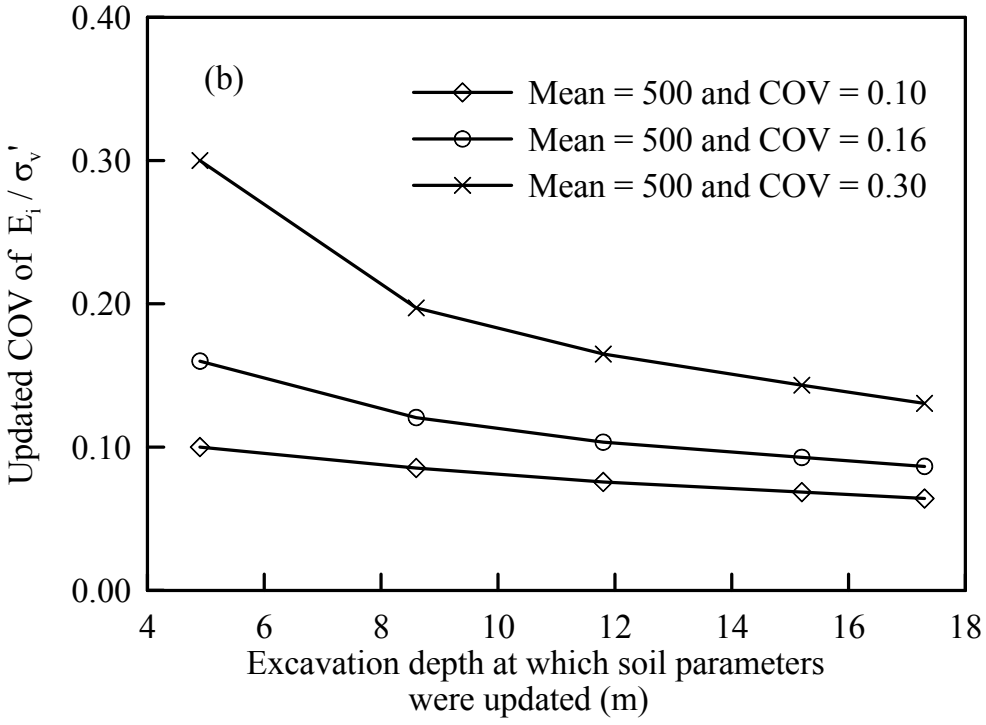

Figure 3.8: Updated COV of soil parameters prior to different stages assuming various COV using Prior distribution 1

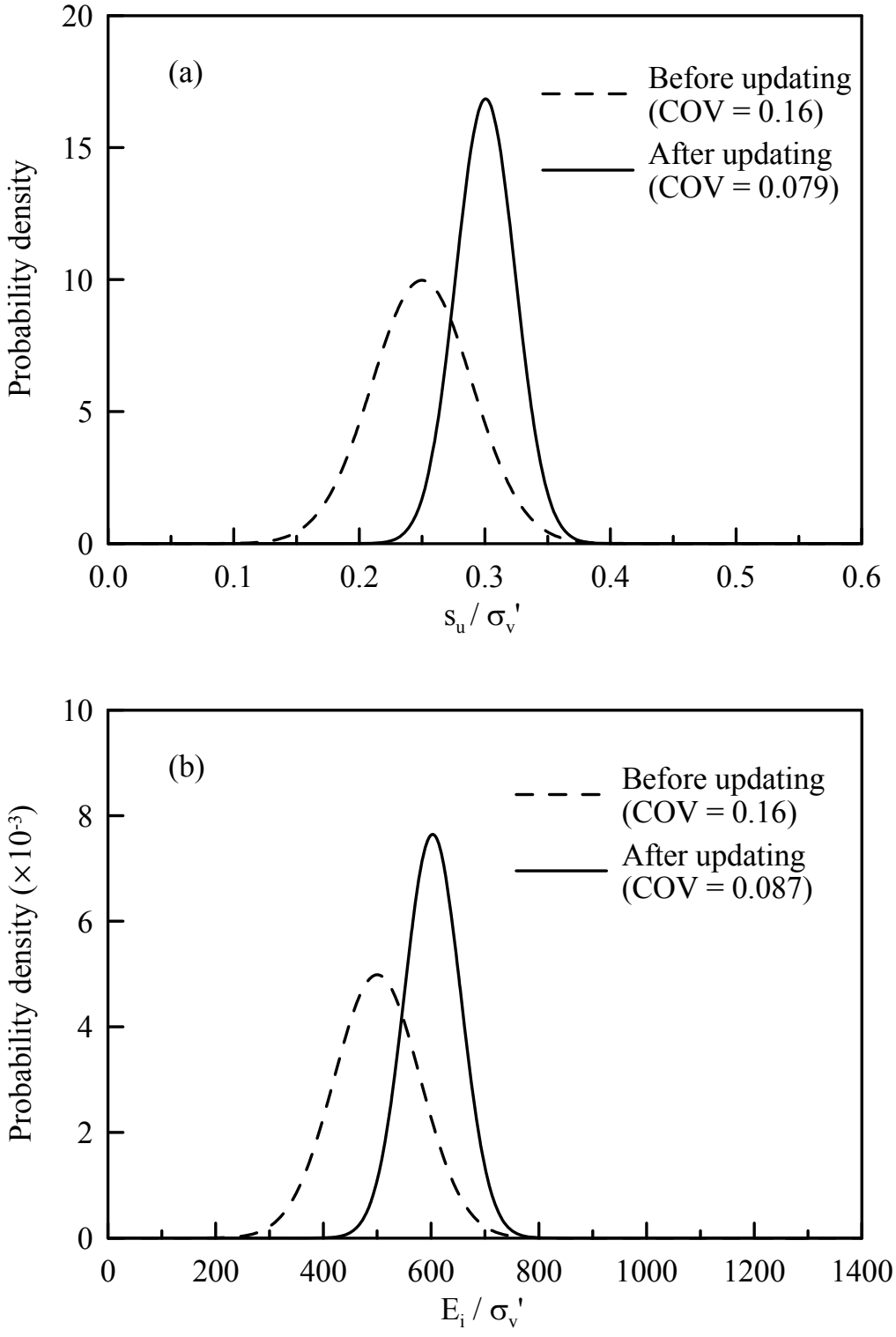

Figure 3.9: Updated distribution of soil parameters prior to final stage of excavation using Prior distribution 1 and COV=0.16

The above results validate the efficiency of using observations to update the prior estimation of soil parameters. Even if the prior estimation is not characterized perfectly initially, the observations during the excavation can "move" the prior estimation to its "true" value through the presented maximum likelihood procedure. Furthermore, with the reduced uncertainties in the input parameters, the uncertainty in the predicted ground and wall responses at the final stage of excavation is further reduced.

Effect of correlation between bias factors of KJHH model

The effect of correlation between the bias factors of the two component models in KJHH model, namely wall deflection model and ground settlement model, is examined in this study. When no information regarding the correlation between the two component models is available, the two bias factors ($\mathbf{c}_h$ and $\mathbf{c}_v$) may simply be assumed uncorrelated, as in the previous analysis ($\rho = 0$). However, the wall deflection and ground settlement in a braced excavation tend to be positively correlated, as reported by Kung et al. (2007).

To investigate the effect of the correlation between $\mathbf{c}_h$ and $\mathbf{c}_v$, the aforementioned back analysis procedure is repeated using Prior distribution 1 with two positive correlation coefficient levels, $\rho = 0.5$ and 0.8. The updated predictions for wall and ground responses with excavation depth at the three levels of correlation (0, 0.5, and 0.8) are shown in Figure 3.10.

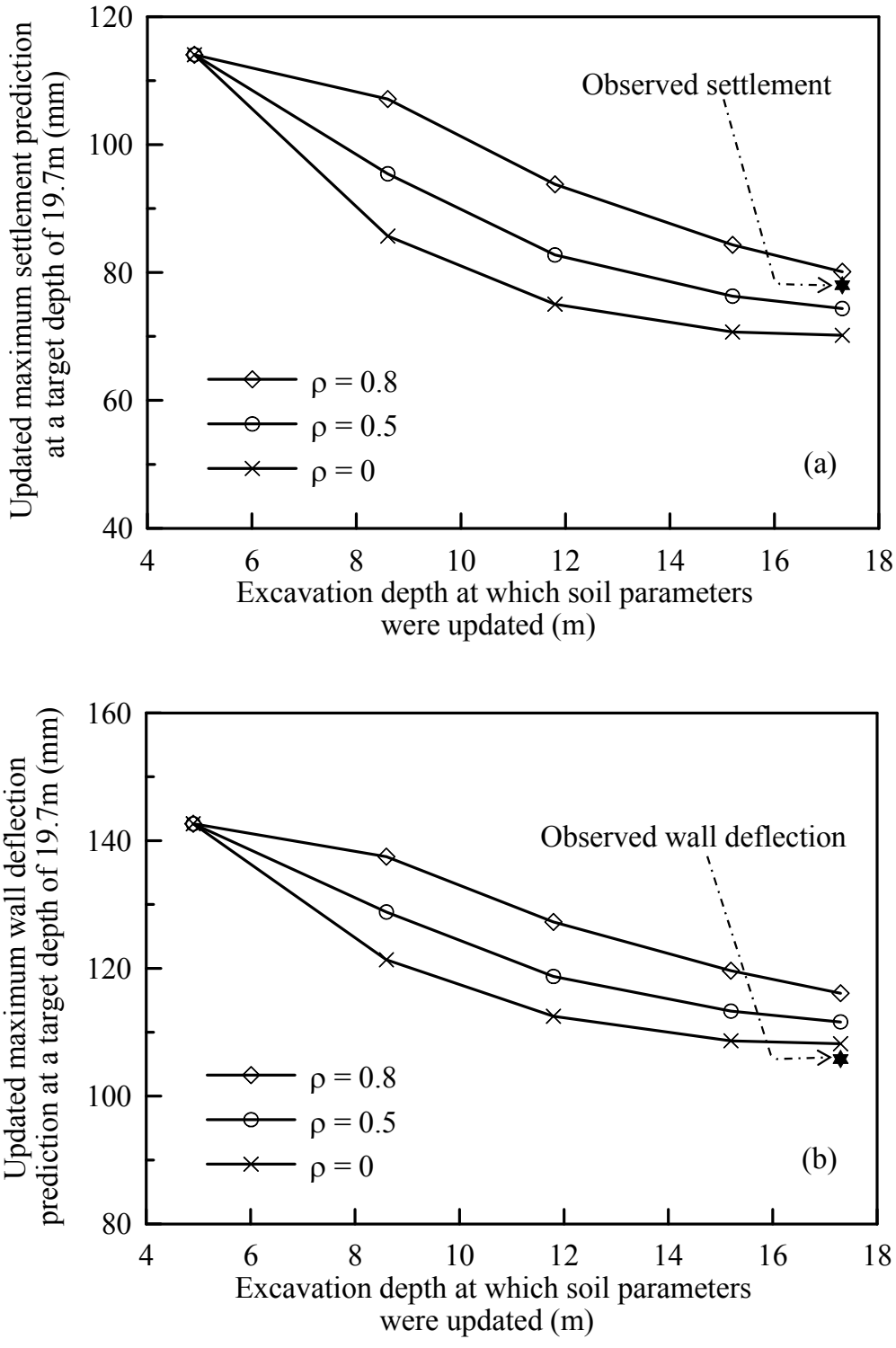

Figure 3.10: Influence of correlation coefficient between model biases on updated predictions using prior distribution 1

The results show that the effect of the correlation between bias factors on the outcome of the developed updating procedure appears to be quite limited. Even with no correlation assumption, the developed procedure for updating soil parameters and predictions is still effective and yields no inferior outcome. Furthermore, this example demonstrates that the developed procedure for probabilistic inverse analysis can be easily adapted to incorporate the known correlation between the model biases of the component models.

Excavation-Induced Damage Potential of Adjacent Buildings

The excavation-induced wall and ground settlement can cause damage to adjacent buildings. Schuster et al. (2009) has developed a framework to evaluate the damage potential of buildings adjacent to the excavation. The basis for this framework is the predicted wall deflection and ground settlement. With the soil parameters being updated during the excavation using the field observations, the predictions of the wall and ground movements are updated. This follows that the prior assessment of building damage potential can be updated with the updated predictions of wall deflection and ground settlement. Thus, updating of the building damage potential is simply an extension of the developed updating scheme for wall and ground movement predictions.

The framework for excavation-induced building damage assessment established by Schuster et al. (2009) includes three components: (1) the profiles of the excavation-induced vertical and lateral ground movements using KJHH model (Kung et al. 2007) and KSJH model (Schuster et al. 2009), respectively; (2) computation of the angular

distortion (β) and lateral strain (ε_l) using the empirical equations; and (3) determination of damage potential index (*DPI*) based on the calculated β and ε_l . The *DPI* is a normalization of the principal strain (Schuster et al. 2009):

$$DPI = 20 \times 10^3 (\varepsilon_l \cos\theta_{\max}^2 + \beta \sin\theta_{\max} \cos\theta_{\max}) \tag{3.13}$$

$$\tan(2\theta_{\max}) = \beta / \varepsilon_l \tag{3.14}$$

where β is angular distortion, ε_l is lateral strain, and $\theta_{\max}$ is direction of crack formation measured from the vertical plane. The *DPI* value ranges between 0 and 100. A smaller *DPI* value indicates a lower damage potential.

In addition to the input parameters that are related to soil conditions ($s_u / \sigma_v^{'}$ and $E_i / \sigma_v^{'}$) and other excavation parameters, the prediction of *DPI* for an adjacent building requires four additional data regarding the properties of the adjacent building. The first is the location of the building, characterized in terms of the distance from the excavation to the adjacent footings (e.g., d_1 and d_2, as shown in Figure 3.11, where d_1 represents the distance from the excavation to the nearest footing and d_2 represents the distance from the excavation to the furthest footing in a building). The second is the embedment depth of the building (D_1 in Figure 3.11). The third is the soil-structure stiffness ratio, $(E_s L^2 / GHb)$, in which E_s is the soil stiffness in the region of footing influence, L is the length of building portion subjected to ground movement, G is the elastic shear modulus of the building, H is the height of the building, and b is the building wall thickness.

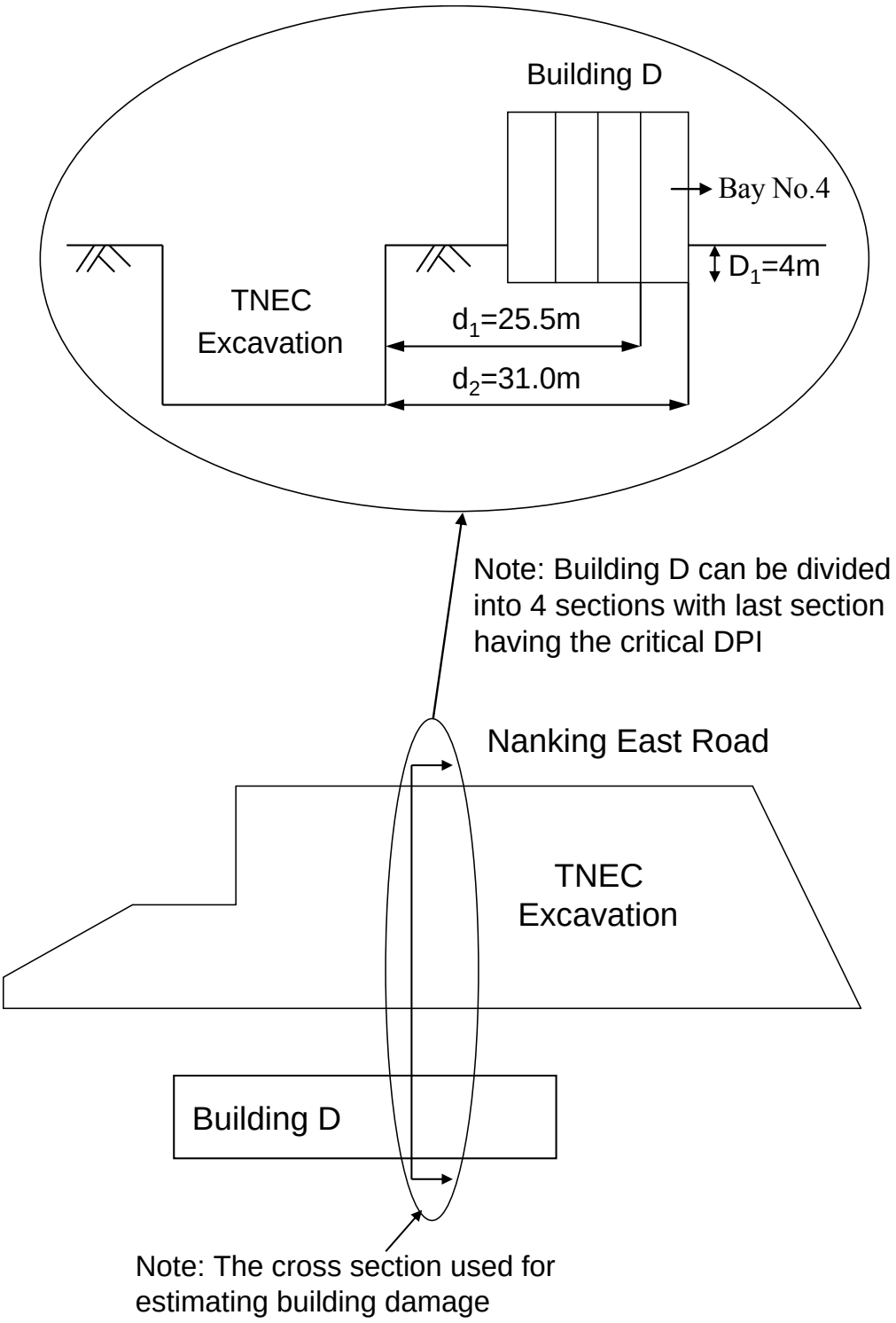

Figure 3.11: Location of excavation and Building D in the TNEC case (adapted from Juang et al. 2011)

For the prediction of *DPI*, the fourth is the structure cracking strain ε_t, which depends on characteristics of a specific building. Detailed parameters for the properties of the adjacent buildings in TNEC case are documented in Schuster et al. (2009). Figure 3.11 shows the layout for Building *D* (Ou et al. 2000) that is adjacent to TNEC excavation. It should be noted that Building *D* could be split up into 4 bays for the purpose of computing *DPI*. As reported by Schuster et al. (2009), Bay No. 4 is identified to be the critical bay (see Figure 3.11) and thus it is selected here as an example to demonstrate the developed procedure for updating of *DPI*.

According to Schuster et al. (2009), the distances from the excavation to the nearest and furthest footings in Bay No. 4 (d_1 and d_2) are 25.5 m and 31.0 m, respectively; the embedment depth of the footing (D_1) is 4 m; the soil-structure stiffness ratio $(E_s L^2 / GHb)$ is estimated to be 15; the structure cracking strain ε_t is estimated to be 0.9. In this study, we follow the procedure by Schuster et al. (2009) to calculate *DPI*. The readers can refer to Schuster et al. (2009) for details.

In this chapter, the soil parameters are updated with the observed settlement and wall deflection. The updated soil parameters are then used to calculate the *DPI* at a target depth of 19.7 m (the final excavation stage). The four prior distributions of $s_u / \sigma_v^{'}$ and $E_i / \sigma_v^{'}$ listed in Table 3.2 are adopted herein. Prior to Stage 3 (the excavation depth at this point is 4.9 m), the predictions of *DPI* for the final stage using the means of the four prior distributions are made and shown in Figure 3.12. After Stage 3 excavation is completed, the observed maximum settlement and wall deflection are used to update the

soil parameters. Then, the updated soil parameters are used to calculate *DPI* at a target excavation depth of 19.7m (final excavation stage), and again, shown in Figure 3.12 (the depth at which this prediction is made is 8.6 m). More and more observations are obtained as the excavation proceeds, and this updating procedure is repeated at excavation depths of 11.8 m, 15.2 m, and 17.3 m.

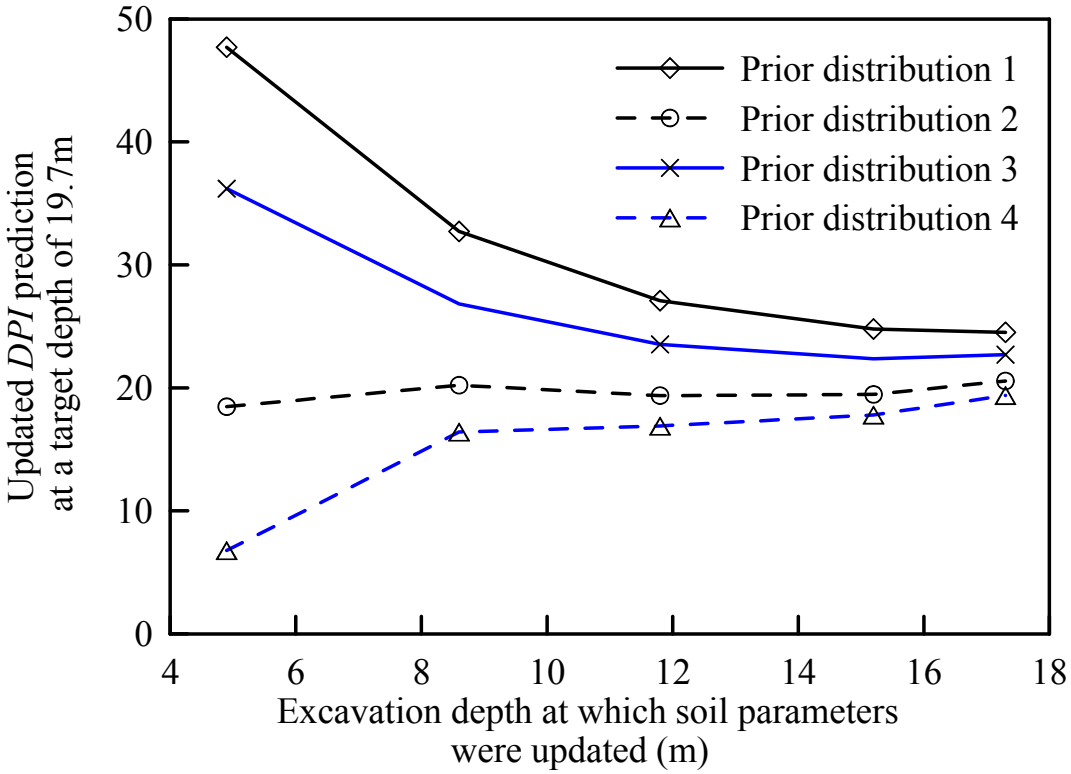

Figure 3.12: Predicted *DPI* of Building D at the target excavation depth of 19.7m with updated soil parameters under various assumptions of prior distribution

Figure 3.12 shows the predictions of the *DPI* at the target depth of 19.7 m (the final stage) using the updated soil parameters prior to Stages 3, 4, 5, 6, and 7(the corresponding depths shown in Figure 3.12 are 4.9 m, 8.6 m, 11.8 m, 15.2 m, and 17.3 m, respectively). As shown in Figure 3.12, the predicted *DPI* values prior to Stage 3 of

excavation differ significantly from each other, as the mean values of those prior distributions are different. With the updated soil parameters, the predictions of *DPI* tend to converge as shown in Figure 3.12. Thus, the updating scheme presented in this chapter is deemed effective for this evaluation of damage potential of an adjacent building. The predicted *DPI* values before the final stage of excavation (the excavation depth at this point is 17.3 m) converge into the range of 19 to 25 among the four prior distributions examined. According to the *DPI* criteria established by Schuster et al. (2009), the building with *DPI* = 19 to 25 would suffer a "slight damage." As reported by Liao (1996) and Ou et al. (2000), the field observations during and after the construction showed that some cracks were found on the internal walls of Bay No. 4 of Building D in the TNEC excavation. This level of building damage would be characterized as "slight damage" according to the evaluation system established by Boscardin and Cording (1989). Thus, the updated prediction of *DPI* and the assessment of building damage are consistent with field observations.

In summary, the case study of TNEC for the wall and ground movements during excavation and their effect on an adjacent building shows that as the soil parameters are updated at each stage based on the observed settlement and wall deflection, the accuracy of the predicted wall and ground movements improves significantly. As a result of the improved predictions of wall and ground movements, the assessment of damage potential of the building adjacent to the excavation becomes more accurate.

Summary

This chapter presents an application of the maximum likelihood approach in the probabilistic inverse analysis in braced excavations. In this approach, the soil parameters ($s_u / \sigma_v^{'}$ and $E_i / \sigma_v^{'}$) are updated with the observed wall and ground responses in a braced excavation. With the updated soil parameters, the predictions of those responses in the subsequent excavation stages and the predicted damage potential of an adjacent building are refined stage by stage. Comparing with the predictions using prior information, the predictions using the updated soil parameters are significantly improved in the case study of TNEC excavation.

Unlike the deterministic inverse analysis, the developed probabilistic inverse analysis approach allows for considerations of the variation in the soil parameters and model bias factors. Accordingly, the updated soil parameters are represented by the posterior distributions. The developed procedure is demonstrated to be effective regardless of the assumed prior distributions of the soil parameters provide that such assumption is within the reasonable range. The efficiency and the effectiveness of this probabilistic analysis approach are illustrated through the case study of TNEC excavation in Taiwan.

CHAPTER FOUR

CONCLUSIONS AND RECOMMENDATIONS

Conclusions

The following conclusions are drawn from the results of the study on the probabilistic back analysis of slope failure presented in Chapter II:

(1) Two procedures for the probabilistic back analysis of slope failure were presented using as an example a recent slope failure case on Freeway No. 3 in Taiwan. The internal friction angle and anchor force are determined to be the key parameters in this case. These two parameters are first back-calculated using the Markov Chain Monte Carlo (MCMC) simulation. The second procedure is based on the maximum likelihood (ML) method. The two procedures yield results that are almost identical. The results indicate that the weakening of the shear strength and deterioration of the anchor system are the primary causes for the Freeway No. 3 slope failure, which is consistent with the field investigations.

(2) Compared with the MCMC simulation based approach, the maximum likelihood based approach is easy to implement in a spreadsheet, requires much less computational effort, and represents a preferred tool for engineering practice. This tool is suitable for use in a post-event failure investigation, and for the evaluation of alternative remedial measures.

(3) The enhanced knowledge of the input parameters for the slope system through back analysis is used to elucidate the failure mechanism and yield a more reasonable estimate of the failure probability of the slope. Selecting a proper remediation method becomes much more certain with the improved knowledge of input parameters coupling with the reliability-based design approach.

The following conclusions are drawn from the results of the study on the probabilistic back analysis of braced excavation presented in Chapter III:

(1) The proposed probabilistic back analysis framework based on maximum likelihood approach is shown effective and efficient for updating key soil parameters in the staged excavation based on either maximum settlement or maximum wall deflection observation or both types of observations. Updating with both type of observation is most efficient overall, and the variation in the predicted wall and ground responses is the smallest when both types of observations are used in the updating.

(2) With the proposed probabilistic back analysis framework, the predictions of excavation-induced ground responses in the subsequent excavation stages and the predicted damage potential of an adjacent building are refined stage by stage. Comparing with the predictions using prior information, the predictions using the updated soil parameters are significantly improved.

(3) The proposed framework is shown effective in improving the responses prediction, regardless of the assumed prior distributions and the levels of the coefficient of variation of the soil parameters. The effect of the correlation between bias factors on the outcome of the proposed framework appears to be quite limited. Even with no correlation assumption, the developed procedure for updating soil parameters and predictions is still effective and yields no inferior outcome.

Recommendations

To further expand the work presented in this thesis, a number of research topics can be undertaken, which include the following:

(1) The analytical model adopted in probabilistic back analysis of slope failure is a simplified limit equilibrium model. It is also advisable to perform the probabilistic back analysis of slope failure combined with the finite element method. The feasibility of using finite element method for slope stability analysis in conjunction with the proposed probabilistic back analysis procedure should be investigated.

(2) The analytical model adopted in probabilistic back analysis of braced excavation is a semi-empirical model called KJHH model. It should be of interest to combine the proposed probabilistic back analysis procedure with

the finite element method for excavation-induced ground response and building damage analysis.

(3) It should be of interest to further investigate the application of the proposed probabilistic back analysis approach in other geotechnical problems such as tunnels, embankments, and geothermal foundations.

APPENDIX A: MAXIMUM LIKELIHOOD FORMULATION

In the maximum likelihood formulation for back analysis of slope failure, the posterior distribution is dependent on both the uncertainty in the observation data and prior information. The prior distribution of input parameters vector $\boldsymbol{\theta}$ is assumed as a multivariate normal distribution, $N(\mu_{\boldsymbol{\theta}}, \mathbf{C}_{\boldsymbol{\theta}})$. When there are M input parameters, the prior joint probability density $f(\boldsymbol{\theta})$ is expressed as (Ang and Tang 2007; Wang et al. 2010):

$$f(\boldsymbol{\theta}) = \frac{1}{\sqrt{(2\pi)^M \mid \mathbf{C}_{\boldsymbol{\theta}} \mid)}} \exp\left[-\frac{1}{2} (\boldsymbol{\theta} - \mu_{\boldsymbol{\theta}})^T \mathbf{C}_{\boldsymbol{\theta}}^{-1} (\boldsymbol{\theta} - \mu_{\boldsymbol{\theta}}) \right] \tag{A.1}$$

Similarly, the probability density function of the observation (Y), given the prior distribution of input parameters, is assumed as a normal distribution, and expressed as:

$$f(Y \mid \boldsymbol{\theta}) = \frac{1}{\sqrt{(2\pi) \mid \sigma_{\varepsilon}^2 \mid)}} \exp\left[-\frac{1}{2} (g(\boldsymbol{\theta}) + \mu_{\varepsilon} - Y)^T \sigma_{\varepsilon}^{-2} (g(\boldsymbol{\theta}) + \mu_{\varepsilon} - Y) \right] \tag{A.2}$$

Based upon the maximum likelihood principle, the posterior probability density $f(\boldsymbol{\theta} \mid Y)$ is proportional to both the prior probability density and the probability density of observation given the prior distribution, which is expressed as (Ledesma et al. 1996a):

$$f(\boldsymbol{\theta} \mid Y) \propto f(Y \mid \boldsymbol{\theta}) \cdot f(\boldsymbol{\theta}) \tag{A.3}$$

The posterior estimator of $\boldsymbol{\theta}$, namely $\boldsymbol{\theta}_d$, is that which maximizes Eq. (A.3),

which is in turn equivalent to minimizing $S(\boldsymbol{\theta}) = -2\ln f(\boldsymbol{\theta} \mid Y)$. When there are two input parameters for the back-analysis, as with our Freeway No. 3 slope, $S(\boldsymbol{\theta})$ remains identical as Eq. (2.6) except the constant terms are disregarded.

REFERENCES

Ang, A.H.S., Tang, W.H. (2007). Probability concepts in engineering: Emphasis on applications to civil and environmental engineering, 2nd ed., Wiley, New York.

Baecher, G.B., Christian, J.T. (2003). Reliability and statistics in geotechnical engineering, Wiley, New York.

Boone, S.J. (1996). Ground-movement-related building damage. Journal of Geotechnical Engineering, 122(11): 886-896.

Boscardin, M.D., Cording, E.J. (1989). Building response to excavation-induced settlement. Journal of Geotechnical Engineering, 115(1):1-21.

Chen, M.M., Wei, C.Y., Fei, L.Y. (2010). Geological analysis for the dip slope slide event of National No. 3 Highway. Journal of Geology, Central Geological Survey of Taiwan, 29(2): 12-15 (in Chinese).

Christian, J.T., Ladd, C.C., Baecher, G.B. (1994). Reliability applied to slope stability analysis. Journal of Geotechnical Engineering, 120 (12): 2180-2207.

Der Kiureghian, A., Liu, P.L. (1986). Structural reliability under incomplete probability information. Journal of Engineering Mechanics, 112(1): 85-104.

Duncan, J.M. (2000). Factors of safety and reliability in geotechnical engineering. Journal of Geotechnical and Environmental Engineering, 126(4): 307-316.

Duncan, J.M., Wright, S.G. (2005). Soil strength and slope stability, Wiley, New York.

Eligehausen, R., Mallée, R., Silva, J.F. (2006). Anchorage in concrete construction, Ernst & Sohn, Berlin.

Eykhoff, P. (1974). System Identification. Parameter and State Estimation, Wiley, New York.

Finno, R.J. (2007). Use of monitoring data to update performance predictions of supported excavations. Theme lecture in the Proceedings, FMGM, International Symposium on Field Measurements in Geomechanics, ASCE, Boston.

Gelman, B.A., Carlin, B.P., Stem, H.S., Rubin, D.B. (2004). Bayesian data analysis. Chapman & Hall, London, 2004.

Gilbert, R.B., Wright, S.G., Liedtke, E. (1998). Uncertainty in back analysis of slopes: Kettleman Hills case history. Journal of Geotechnical and Environmental Engineering, 124(12): 1167-1176.

Harr, M.E. (1987). Probability-based design in civil engineering, McGraw-Hill Book Company, New York.

Hashash, Y.M.A., Jung, S., Ghaboussi, J. (2004). Numerical implementation of a neural network based material model in finite element analysis. International Journal for Numerical Methods in Engineering, 59(7): 989-1005.

Hashash, Y.M.A., Marulanda, C., Ghaboussi, J., Jung, S. (2006). Novel approach to integration of numerical modeling and field observations for deep excavations. Journal of Geotechnical and Geoenvironmental Engineering, 132(8): 1019-1031.

Hastings, W.K. (1970). Monte Carlo sampling methods using Markov chains and their applications. Biometricka, 57: 97-109.

Hoek, E., Bray, J. (1981). Rock slope engineering, 3rd ed., Institution of Mining and Metallurgy, London.

Hoek, E. (2006). Practical rock engineering. Chapter 7: A slope stability problem in Hong Kong; and Chapter 8: Factor or safety and probability of failure. In: http://www.rocscience. com/hoek/PracticalRockEngineering.asp.

Honjo, Y., Liu, W.T., Soumitra, G. (1994). Inverse analysis of an embankment on soft clay by extended Bayesian method. International Journal for Numerical and Analytical Methods in Geomechanics, 18: 709-734.

Hsiao, E.C.L., Schuster, M., Juang, C.H., Kung, G.T.C. (2008). Reliability analysis of excavation-induced ground settlement for building serviceability evaluation. Journal of Geotechnical and Geoenvironmental Engineering, 134(10): 1448-1458.

Hsiao, C.Y., Hsieh, P.S., Chi, S.Y. (2011). Preliminary study using unconventional photogrammetry to evaluate the earthwork volume – a case study of the landslide occurred on the Cidu Section of Formosan Freeway. Journal of Chinese Soil and Water Conservation, 42 (2): 120-130 (in Chinese).

Juang, C.H., Jhi, Y.Y., Lee, D.H. (1998). Stability analysis of existing slopes considering uncertainty. Engineering Geology, 49 (2): 111-122.

Juang, C.H., Schuster, M., Ou, C.Y., Phoon, K.K. (2011). Fully-probabilistic framework for evaluating excavation-induced building damage potential. Journal of Geotechnical and Geoenvironmental Engineering, 137(2): 130-139.

Juang, C.H., Luo, Z., Atamturktur, S., Huang, H. (2013). Bayesian updating of soil parameters for braced excavations using field observations. Journal of Geotechnical and Geoenvironmental Engineering, 139(3): 395-406.

Kung, T.C. (2003). Surface settlement induced by excavation with consideration of small strain behavior of Taipei silty clay. Ph.D. thesis, Dept. of Construction Engineering, National Taiwan Univ. of Science and Technology, Taipei, Taiwan.

Kung, G.T.C., Juang, C.H., Hsiao, C.L., Hashash, Y.M.A. (2007). Simplified model for wall deflection and ground surface settlement caused by braced excavation in clays. Journal of Geotechnical and Geoenvironmental Engineering, 133(6): 731-747.

Ledesma, A., Gens, A., Alonso, E.E. (1996a). Parameter and variance estimation in geotechnical back analysis using prior information. International Journal for Numerical and Analytical Methods in Geomechanics, 20:119-141.

Ledesma, A., Gens, A., Alonso, E.E. (1996b). Estimation of parameters in geotechnical back analysis - I. Maximum likelihood approach. Computers and Geotechnics, 18(1):1-27.

Lee, Y.F., Chi, Y.Y., Juang, C.H., Lee, D.H. (2012). Reliability analysis of rock wedge stability – a Knowledge-based Clustered Partitioning (KCP) approach. Journal of Geotechnical and Environmental Engineering, 138(6): 700-708.

Levasseur, S., Malécot, Y., Boulon, M., Flavigny, E. (2008). Soil parameter identification using a genetic algorithm. International Journal for Numerical and Analytical Methods in Geomechanics, 32(2):189-213.

Li, J., Tham, L.G., Junaideen, S.M., Yue, Z.Q., Lee, C.F. (2007). Loose fill slope stabilization with soil nails: Full-scale test. Journal of Geotechnical and Environmental Engineering, 134(3): 277-288.

Li, D.Q., Chen, Y.F., Lu, W.B., Zhou, C.B. (2011). Stochastic response surface method for reliability analysis of rock slopes involving correlated non-normal variables. Computers and Geotechnics, 38(1): 58-68.

Liao, J.T. (1996). Performance of a top down deep excavation. Ph.D. thesis, Dept. of Construction Engineering, National Taiwan Univ. of Science and Technology, Taipei, Taiwan.

Lin, H.H., Shen, C.S., Chi, C.C. (2010). Landforms interpretation and analysis for the dip slope slide event of National No. 3 Highway. Journal of Geology, Central Geological Survey of Taiwan, 29(2): 20-23 (in Chinese).

Metropolis, N., Rosenbluth, A.W., Rosenbluth, M.N., Teller, A.H., Teller, E. (1953). Equations of state calculations by fast computing machines. Journal of Chemical Physics, 21(6): 1087-1092.

Najjar, S.S., Gilbert, R.B. (2009). Importance of lower-bound capacities in the design of deep foundations. Journal of Geotechnical and Geoenvironmental Engineering, 135(7): 890-900.

Ou, C.Y., Tang, Y.G. (1994). Soil parameter determination for deep excavation analysis by optimization. Journal of the Chinese Institute of Engineers, 17(5): 671-688.

Ou, C.Y., Liao, J.T., Lin, H.D. (1998). Performance of diaphragm wall constructed using top-down method. Journal of Geotechnical and Geoenvironmental Engineering, 124(9): 798-808.

Ou, C.Y., Liao, J.T., Cheng, W.L. (2000). Building response and ground movements induced by a deep excavation. Geotechnique, 50(3): 209-220.

Park, J.K., Gardoni, P., Biscontin, G. (2010). Estimation of soil properties and deformation in staged constructions based on MCMC method. GeoFlorida 2010: Advances in Analysis, Modeling & Design, GSP 199, ASCE, p.1885-1894.

Park, H.J., West, T.R., Woo, I. (2005). Probabilistic analysis of rock slope stability and random properties of discontinuity parameters, Interstate Highway 40. Engineering Geology, 79(3-4): 230-250.

Park, H.J., Um, J.G., Woo, I., Kim, J.W. (2012a). Application of fuzzy set theory to evaluate the probability of failure in rock slopes. Engineering Geology, 125: 92-101.

Park, H.J., Um, J.G., Woo, I., Kim, J.W. (2012b). The evaluation of the probability of rock wedge failure using the point estimate method. Environmental Earth Sciences, 65: 353-361.

Peck, R.B. (1969). Advantages and limitations of the observational method in applied soil mechanics. Geotechnique, 19(2): 171-187.

Penalba, R.F., Luo, Z., Juang, C.H. (2009). Framework for probabilistic assessment of landslide: A case study of EI Berrinche. Environmental Earth Sciences, 59 (3): 489-499.

Phoon, K.K., Kulhawy, F.H. (1999). Characterization of geotechnical variability. Canadian Geotechnical Journal, 129(4): 612-624.

Phoon, K.K., Kulhawy, F.H. and Grigoriu, M.D. (2003). Multiple resistance factor design for shallow transmission line structure foundations. Journal of Geotechnical and Geoenvironmental Engineering, 129(9): 807-818.

Schuster, M., Kung, G.T.C., Juang, C.H., Hashash, Y.M.A. (2009). Simplified model for evaluating damage potential of buildings adjacent to a braced excavation. Journal of Geotechnical and Geoenvironmental Engineering, 135(12): 1823-1835.

Shou, K.J., Chen, Y.L. (2005). Spatial risk analysis of Li-shan landslide in Taiwan. Engineering Geology, 80(3-4): 199-213.

Stark, T.D., Newman, E.J., Aust, R.A. (2008). Back-analysis of PVC geomembrane lined pond failure. Geosynthetics International Journal, 15(4): 258-268.

Taiwan Geotechnical Society. (2011). Summary report of investigation of reasons for Taiwan Freeway No.3 (Formosan Freeway Cidu Section) 3k+300m Landslide. Rep. Prepared by Taiwan Geotechnical Society for Ministry of Transportation and Communication, Taiwan (in Chinese).

Tang, W.H., Stark, T.D., Angulo, M. (1999). Reliability in back analysis of slope failures. Soils and Foundations, 39(5): 73-80.

Tang, Y.G., Kung, G.T.C. (2009). Application of nonlinear optimization technique to back analyses of deep excavation. Computers and Geotechnics, 36(1-2): 276-290.

Tang, Y.G., Kung, G.T.C. (2010). Investigating the effect of soil models on deformations caused by braced excavations through an inverse-analysis technique. Computers and Geotechnics, 37(6): 769-780.

Tarantola, A. (2005). Inverse problem theory and methods for model parameter estimation, 2nd Ed., Elsevier Science, New York.

Turner, A.K., Schuster, R.L. (1996). Landslides — Investigation and mitigation: National Research Council, Transportation Research Board Special Report 247, National Academy Press, Washington, D.C.

Wang, J.P., Huang, D. (2012). Rosenpoint: A Microsoft Excel-based program for the Rosenblueth point estimate method and an application in slope stability analysis. Computers and Geosciences, 48: 239-243.

Wang, L., Luo, Z., Juang, C.H. (2013). Updating uncertain soil parameters by maximum likelihood method for predicting maximum ground and wall movements in braced excavations. Foundation Engineering in the Face of Uncertainty, GSP 229, ASCE, pp. 530-541.

Wang, Y., Au, S.K., Cao, Z. (2010). Bayesian approach for probabilistic characterization of sand friction angles. Engineering Geology, 114(3-4): 354-363.

Wang, Y., Cao, Z., Au, S.K. (2010). Efficient mote Carlo simulation of parameter sensitivity in probabilistic slope stability analysis. Computers and Geotechnics, 37(7-8): 1015-1022.

Wu, T.H., Tang, W.H., Sangrey, D.A., Baecher, G.B. (1989). Reliability of offshore foundations — State-of-the-art. Journal of Geotechnical Engineering, 115(2): 157-178.

Wu, T.H. (2011). 2008 Peck Lecture: The observational method: case history and models. Journal of Geotechnical and Geoenvironmental Engineering, 137(10): 862-873.

Wyllie, D.C., Mah, C.W. (2004). Rock slope engineering, 4th Ed., Spon Press, London.

Xanthakos, P. (1991). Ground Anchors and Anchored Structures, Wiley, New York.

Zhang, L.L., Zhang, L.M., Tang, W.H. (2009). Uncertainty of field pullout resistance of soil nails. Journal of Geotechnical and Geoenvironmental Engineering, 135(7): 966-972.

Zhang, L.L., Zhang, J., Zhang, L.M., Tang, W.H. (2010a). Back analysis of slope failure with Markov chain Monte Carlo simulation. Computers and Geotechnics, 37(7-8): 905-912.

Zhang, J., Tang, W.H., Zhang, L.M. (2010b). Efficient probabilistic back-analysis of slope stability model parameters. Journal of Geotechnical and Geoenvironmental Engineering, 136(1): 99-109.

Zhang, J., Zhang, L.M., Tang, W.H. (2011). Slope reliability analysis considering site-specific performance information. Journal of Geotechnical and Geoenvironmental Engineering, 137(3): 227-238.